Title:

Phosphatidylserine prevents the generation of a protein-free giant plasma membrane domain in yeast

Authors:

Tetsuo Mioka[1*], Guo Tian[1], Wang Shiyao[1], Takuma Tsuji[2], Takuma Kishimoto[1], Toyoshi Fujimoto[2], and Kazuma Tanaka[1*]

Author affiliations:

[1] Division of Molecular Interaction, Institute for Genetic Medicine, Hokkaido University Graduate School of Life Science, Sapporo, Hokkaido, Japan

[2] Laboratory of Molecular Cell Biology, Research Institute for Diseases of Old Age, Juntendo University Graduate School of Medicine, Tokyo, Japan.

*Corresponding author: Tetsuo Mioka and Kazuma Tanaka

E-mail: mioka@igm.hokudai.ac.jp (TM) and k-tanaka@igm.hokudai.ac.jp (KT)

Abstract

Membrane phase separation accompanied with micron-scale domains of lipids and proteins occurs in artificial membranes; however, a similar large phase separation has not been reported in the plasma membrane of the living cells. We demonstrate here that a stable micron-scale protein-free region is generated in the plasma membrane of the yeast mutants lacking phosphatidylserine. We named this region the "void zone". Transmembrane proteins, peripheral membrane proteins, and certain phospholipids are excluded from the void zone. The void zone is rich in ergosterol and requires ergosterol and sphingolipids for its formation. These characteristics of the void zone are similar to the properties of the liquid-ordered domain caused by phase separation. We propose that phosphatidylserine prevents the formation of the void zone by preferentially interacting with ergosterol. We also found that void zones were frequently in contact with vacuoles, in which a membrane domain was also formed at the contact site.

Introduction

The fluid mosaic model describing the dynamic distribution of proteins at the plasma membrane has been largely modified and developed to date (Singer and Nicolson, 1974; Nicolson, 2014; Kusumi A *et al.,* 2012). Lateral diffusion of proteins is not free and is influenced by protein interaction with other plasma membrane proteins and cytoskeletal elements. In cholesterol-rich domains, such as lipid rafts, certain proteins can accumulate due to protein-protein or protein-lipid interactions (Lingwood and Simons, 2010). The plasma membrane is currently considered to be a nanoscale heterogeneous structure. In addition, several macroscopic diffusion barriers have been detected, and some of the barriers represent membrane compartmentalization due to interactions between the cytoskeleton and membrane

proteins (Kusumi *et al.,* 2012; Trimble and Grinstein, 2015). In artificial membranes, such as giant unilamellar vesicles (GUVs) and giant plasma membrane vesicles (GPMVs), membrane phase separation leads to the formation of even larger domains of proteins and lipids (Veatch and Keller, 2003; Baumgart *et al.,* 2007; Elson *et al.,* 2010; Carquin *et al.,* 2016). In phase-separated membranes, two domains coexist: a liquid-ordered phase (Lo), rich in sterols and saturated lipids, and a liquid-disordered phase (Ld), where unsaturated lipids are distributed. Phase separation in artificial membranes has been well studied and is often compared to the nanoscale membrane domains found in the cells; however, large-scale phase separation is not observed in the plasma membranes of the living cells due to unknown reasons.

The plasma membranes are composed of diverse lipid species, and the role of phosphatidylserine (PS) and phosphatidylinositol phosphates (PIPs) in various cellular functions has been studied (Uchida *et al.,* 2011; Cho *et al.,* 2015; Middel *et al.,* 2016; Tsuchiya *et al.,* 2018; Michell, 2008; Balla, 2013). However, it is poorly understood how individual phospholipids influence the membrane environment.

Although PS is essential for growth of mammalian cells, yeast mutant cells lacking *CHO1*, the only PS synthase in the budding yeast, can grow (Arikketh *et al.,* 2008; Atkinson *et al.,* 1980). To explore a new role for PS, we have analysed PS-deficient *cho1*Δ yeast cells. In this study, we show that stable large protein-free membrane domains are detected in the plasma membrane of PS-deficient *cho1*Δ cells, which we named the "void zone". Transmembrane proteins, peripheral membrane proteins, and certain phospholipids are excluded from the void zone. This property is very similar to the Lo phase in the phase-separated artificial membranes. Our results suggest that PS suppresses the development of large-scale phase separation in the plasma membrane of the living cells and consequently ensures the distribution of proteins and lipids throughout the plasma membrane. Furthermore, we found that vacuoles, the lysosomal organelle of yeast, contact with the void zone on the plasma

membrane.

Results

PS-deficient cells show a protein-free region, "void zone", in the plasma membrane.

GFP-Snc1-pm, a mutant of v-SNARE Snc1, is uniformly distributed throughout the plasma membrane due to a defect in its endocytosis (Lewis *et al.* 2000). In PS-deficient *cho1*Δ cells grown at 37°C, GFP-Snc1-pm was heterogeneously distributed on the plasma membrane (Figure 1A). A GFP-Snc1-pm-deficient region was barely detectable at 30°C, was frequently present during incubation at 37°C for over 6 hours, and was not detected after heat shock at 42°C for 20 min (Figure 1B). This Snc1-pm-deficient region of the plasma membrane is referred to as "void zone" in the present study. The shape of the void zone observed on the cell surface was irregular and did not correspond to a smooth circle, and some cells had multiple void zones (Figure 1C). When *cho1*Δ cells were observed immediately after staining with FM4-64 lipophilic dye, FM4-64 was distributed throughout the plasma membrane including the void zone (Figure 1D), suggesting that the plasma membrane is not lost or significantly damaged in cells harbouring the void zone. To examine whether the void zone influences the distribution of other transmembrane proteins, four different transmembrane proteins, Pma1, Pdr5, Pdr12, and Sfk1, were compared with Snc1-pm (Figure 1E). Pma1 is the major plasma membrane H^+-ATPase (Serrano *et al.*, 1986). Pdr5 and Pdr12 are the ATP-binding cassette (ABC) transporters involved in the multidrug resistance and the weak organic acid resistance, respectively (Bauer *et al.*, 1999). Sfk1 regulates phospholipid asymmetry in conjunction with the flippase complex Lem3-Dnf1/2 and is involved in proper localization of a phosphatidylinositol-4-kinase Stt4 (Audhya and Emr, 2002; Mioka *et al.*, 2018). The results indicate that all these proteins showed void zones in the same region with void zones detected by Snc1-pm; the percentage of overlapping void zones was more than 82% in all cases

(Figure 1E; percentage was determined from 70-110 cells with void zones). These results suggest that the void zone is a membrane protein-free region common to all other membrane proteins (see below), and the void zone can represent an abnormal lipid domain that inhibits the lateral movement of the transmembrane proteins into the domain.

We also investigated the distribution of eisosomes, large immobile protein complexes that form furrow-like invaginations in the fungal plasma membrane (Douglas and Konopka, 2014). Eisosome components, Pil1 and Sur7, were not distributed in the void zone (Figure 1—figure supplement 1). The void zone was also devoid of the eisosome structure.

To further examine whether transmembrane proteins are completely absent in the void zone, electron microscopy combined with the freeze-fracture replica method was applied (Fujita *et al.*, 2010; Tsuji *et al.*, 2017). In this method, transmembrane proteins are detected as the granular structures called intramembrane particles (IMPs) (Figure 1F). In the protoplasmic face of the plasma membrane in *cho1*Δ cells, most of the regions were IMP-rich although a submicron-sized smooth region without IMPs was detectable (Figure 1G). To examine whether this IMP-deficient area is the void zone, we labelled Pma1-GFP with an anti-GFP antibody and colloidal gold-conjugated protein A (Figure 1F). As expected, only the IMP-rich area was stained for Pma1-GFP and there was no labelling in the IMP-deficient area (Figure 1H). This result is consistent with the fluorescence microscopy images (Figure 1E) and indicates that the void zone corresponds to the IMP-deficient area. Thus, there are no transmembrane proteins in the void zone.

Figure 1

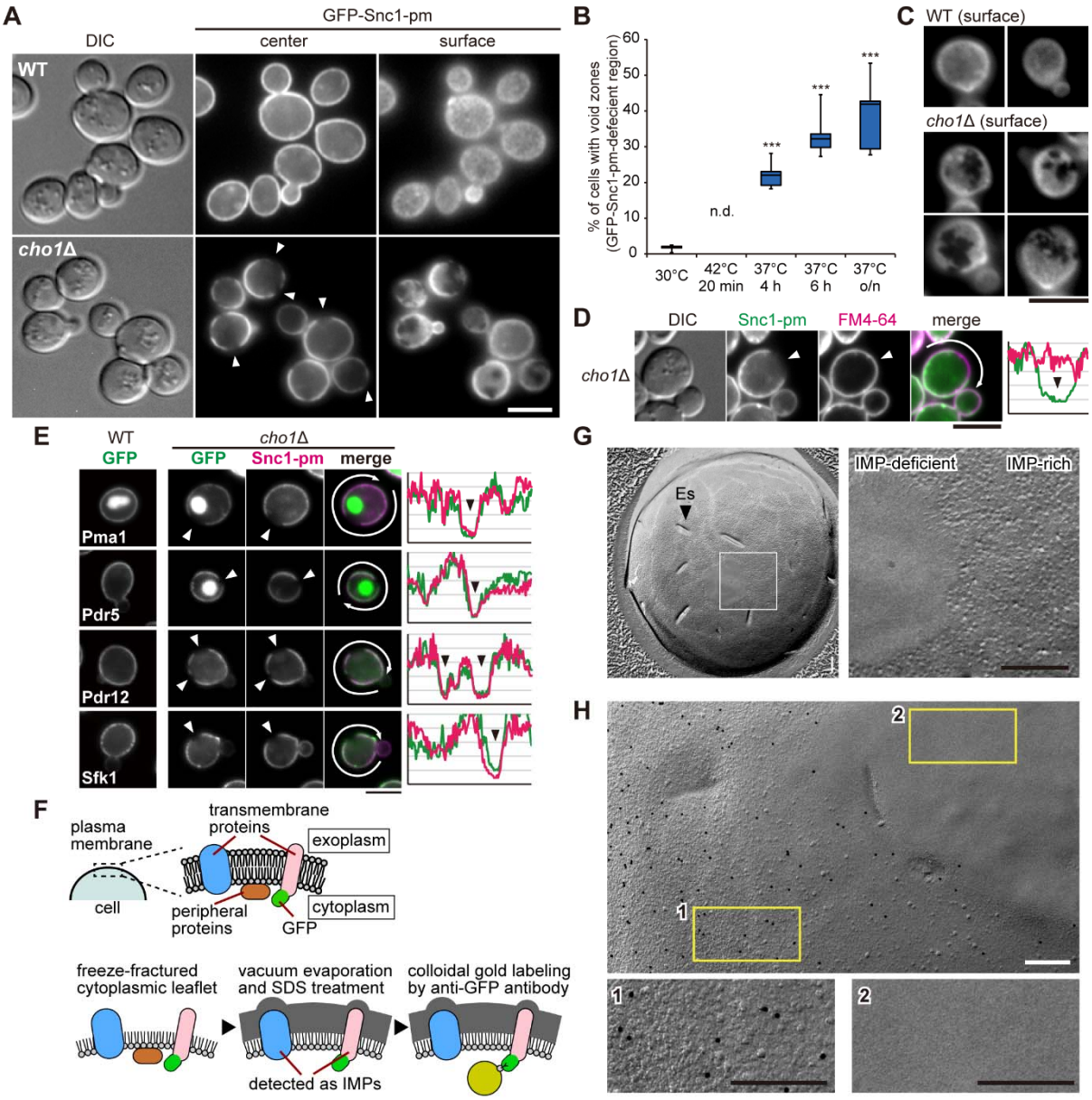

Figure 1 A protein-free region, void zone, is present in the plasma membrane of the PS-deficient yeast cells

(A) Representative images of the void zone. Cells expressing GFP-Snc1-pm were grown overnight in YPDA medium at 37°C. Arrowheads indicate the void zone. Scale bar: 5 μm. (B) The percentage of cells with the void zone. *cho1*Δ cells expressing GFP-Snc1-pm were grown under the indicated conditions. The incidence of the void zone was examined (n > 100 cells, five independent experiments) and is shown as a box plot. Asterisks indicate significant

differences from the data obtained at 30°C according to the Tukey–Kramer test (***, $p < 0.001$; n.d., not detected). (C) Representative images of the void zone in the cell surface. Cells were prepared as in (A). Scale bar: 5 μm. (D) The lipophilic dye FM4-64 can be distributed in the void zone. *cho1*Δ cells were prepared as in (A) and stained with FM4-64 just before the observation. Fluorescence intensities of GFP-Snc1-pm and FM4-64 around the cell (arrows) are plotted on the right. Arrowheads indicate the void zone. Scale bar: 5 μm. (E) The void zone is common to various transmembrane proteins. Cells expressing the indicated proteins were prepared as in (A). Arrowheads indicate the void zone. Fluorescence intensities around the cell (arrows) were plotted as in (D). Scale bar: 5 μm. (F) A scheme of freeze-fracture replica labelling method. (G, H) Freeze-fracture EM images of the plasma membrane of *cho1*Δ cells (G) or Pma1-GFP-expressing *cho1*Δ/P_{GAL1}-*CHO1* diploid cells (H). Cells were grown at 37°C. The enlarged image of the area indicated by the square is shown on the right (G) or at the bottom (H). Colloidal gold particles indicate Pma1-GFP labelled by anti-GFP antibody (H). Scale bars: 0.2 μm. (IMP, intramembrane particles; Es, eisosome)

Figure 1 S1

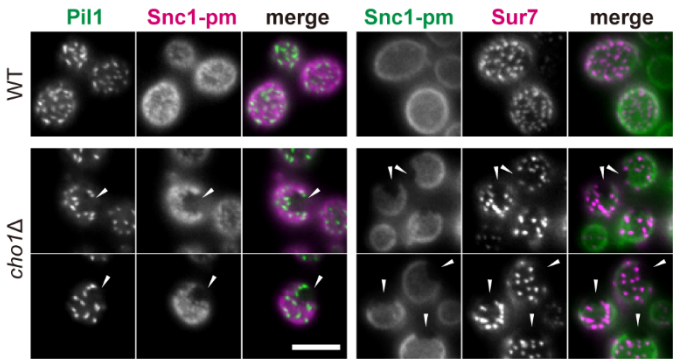

Figure 1-Figure supplement 1. Eisosome structures are excluded from the void zone

Eisosome components were not present in the void zone. Cells expressing Pil1-GFP and mRFP-Snc1-pm or GFP-Snc1-pm and Sur7-mRFP were grown in YPDA medium at 37°C. Images shown are focused on the cell surface. Arrowheads indicate the void zone. Scale bar: 5 μm.

Characterization of the dynamics of the void zone.

We next examined the stability of the void zone by time-lapse imaging. Most of the void zones were detected over tens of minutes, and some void zones were detectable for longer period of time over 90 min. Bud growth and cytokinesis appeared to proceed normally in the void zone-containing cells (Figure 2A). Consistently, *cho1*Δ cells showed no significant growth defects at 37°C compared to growth at 30°C (Figure 2B). These results suggest that the void zone is a very stable lipid domain, which does not influence cell cycle progression. On the other hand, the void zone was essentially undetectable in a saturated culture with high cell density and very low cell growth. Thus, we investigated whether the frequency of the void zone formation is associated with the growth phase (Figure 2C). Yeast cells show rapid growth in the presence of abundant carbon sources such as glucose. When glucose is depleted, the cells switch to a slower growth rate using ethanol as a metabolic carbon source via a diauxic shift and consequently enter the stationary phase (Gray *et al.,* 2004). As shown in

Figure 2C, the frequency of the void zone detection was increased early in the logarithmic growth phase and began to decrease starting from the middle phase. Remarkably, the void zone rapidly disappeared when the cells entered the diauxic shift, and no changes were observed after 12 hours, suggesting that the void zone is formed and maintained only in the presence of abundant carbon sources. To investigate the disappearance of the void zone, we examined whether certain stresses induce the disappearance. *cho1*Δ cells grown at 37°C were incubated for additional 3 h at 37°C under three stress conditions, including ATP depletion, glucose starvation, and translation inhibition; then, the cell numbers and the frequency of the void zone were measured. Cell growth was almost completely blocked by all these stresses, and the frequency of the void zone detection was significantly reduced by ATP depletion and glucose starvation, but not by translation inhibition (Figure 2D). These results suggest that the maintenance of the void zone is energy-dependent and does not necessarily require cell growth.

We also noticed that the void zone tends to occur in the mother cells rather than the daughter cells (Figure 2E). To confirm this, the distribution of the void zone was categorized into the following groups; cells with no bud or small bud (type 1), cells with mid-large bud in which the void zone occurs only in the mother cell (type 2), and cells in which the void zone occurs in the mother and daughter cells (type 3). As a result, almost all void zones appeared only in the mother cells before or during budding (type 1 and 2); very few type 3 cells were detected, and no cells with void zones formed only in the daughter cells were observed (Figure 2E). This biased distribution was observed even under the condition of OD_{600} = 4.0-6.0, which shows high frequency of the void zone. Exocytosis and endocytosis frequently occur in a bud, which is a polarized growth site, compared to a mother cell. These results suggest that the void zone is generated in a more static membrane.

Figure 2

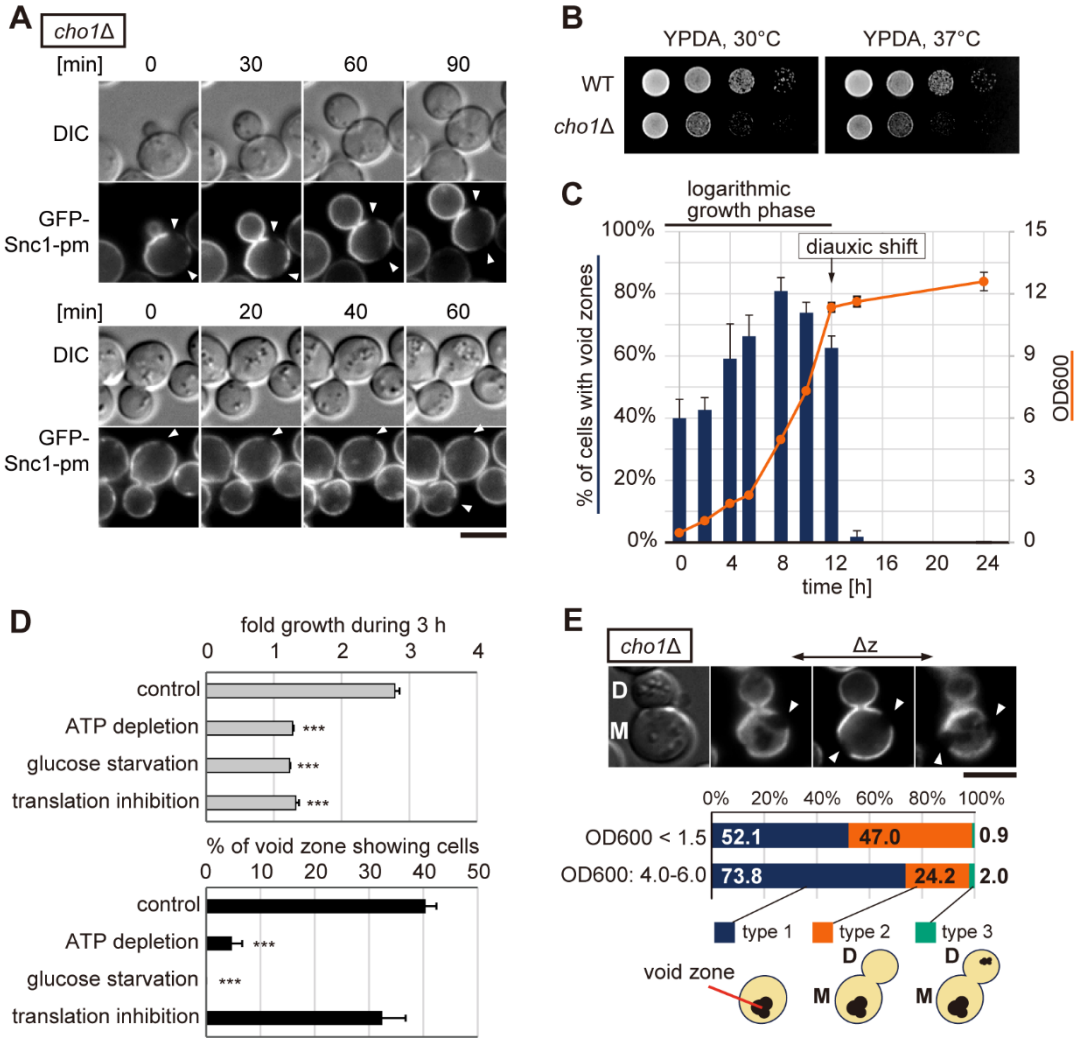

Figure 2 The void zone is stably maintained in an energy-dependent manner

(A) Time-lapse imaging of the void zone. *cho1*Δ cells expressing GFP-Snc1-pm were grown in YPDA medium at 37°C. Two representative examples are shown; a cell with a growing bud (upper panels) and a dividing cell (lower panels) with the void zones. Arrowheads indicate the void zone. Scale bar: 5 μm. (B) Normal growth of *cho1*Δ cells at 37°C. Serial dilutions of cultures were spotted onto the YPDA plates followed by incubation at 30°C or 37°C for 1 d. (C) Frequency of the void zone generation at various growth stages. *cho1*Δ cells expressing GFP-Snc1-pm were grown in YPDA at 37°C, and the percentage of the cells with void zones (blue bars) and the OD_{600} (orange line) were determined. Data of three independent experiments (n > 100 cells each) are shown as the mean and SD. (D)

Disappearance of the void zone under stress conditions. *cho1*Δ cells expressing GFP-Snc1-pm were grown to the early log phase at 37°C and were shifted to YPDA medium containing 20 mM sodium azide (ATP depletion), YPA medium lacking glucose (glucose starvation), and YPDA medium containing 10 μg/ml cycloheximide (translation inhibition). After incubation for 3 h at 37°C, OD_{600} and the incidence of the void zone (n > 100 cells) were determined. Data of three independent experiments are shown as the mean and SD. Asterisks indicate significant differences determined by the Tukey–Kramer test (***, $p < 0.001$). (E) Biased formation of the void zone in the mother cell. *cho1*Δ cells expressing GFP-Snc1-pm were prepared as in (A). A representative pattern of the void zone taken on the different Z focal planes is shown in the upper panel; the void zone occurs in the mother cell (M) but not in the daughter cell (D). Arrowheads indicate the void zone. Scale bar: 5 μm. The percentage of the cells with the void zone in the indicated pattern types (n > 200 cells each) is shown in the lower panel.

Void zone formation is specific to PS-depletion and is a reversible process.

To examine whether the void zone can be detected in the lipid mutants other than *cho1*Δ, we investigated the mutants of the genes involved in the synthesis of phosphatidylethanolamine (PE) and phosphatidylcholine (PC). In PE-, and PC-deficient cells, GFP-Snc1-pm was evenly distributed in the plasma membrane, and the void zone was not detected (Figure 3A). We next examined whether the recovery of PS levels dissipates the void zone by adding lyso-PS to the culture media. Incorporated lyso-PS is rapidly converted to PS in the endoplasmic reticulum (ER) via a *CHO1*-independent pathway (Fairn *et al.,* 2011; Maeda *et al.,* 2013). The recovery of PS was verified by expressing a PS-specific biosensor Lact-C2 (Yeung *et al.,* 2008). In *cho1*Δ cells without lyso-PS, the frequency of the void zone did not change for 60 min and mRFP-Lact-C2 remained diffuse in the cytosol. On the other hand, the addition of lyso-PS

224 significantly reduced the incidence of the void zone and resulted in the localization of mRFP-
225 Lact-C2 to the plasma membrane (Figure 3B). These results indicate that the void zone
226 formation is a reversible process. After the addition of lyso-PS, void zones did not disappear
227 uniformly, but rather appeared to be gradually repaired from the boundaries (Figure 3C). In
228 some *cho1*Δ cells, mRFP-Lact-C2 was distributed outside of the void zone (Figure 3D). This
229 void zone is gradually repaired by PS around the void zone. Our results suggest that the void
230 zone is a lipid domain that consists of a lipid (lipids), and random distribution of these lipids
231 in the plasma membrane is facilitated by interaction with PS.
232

233 **Figure 3**

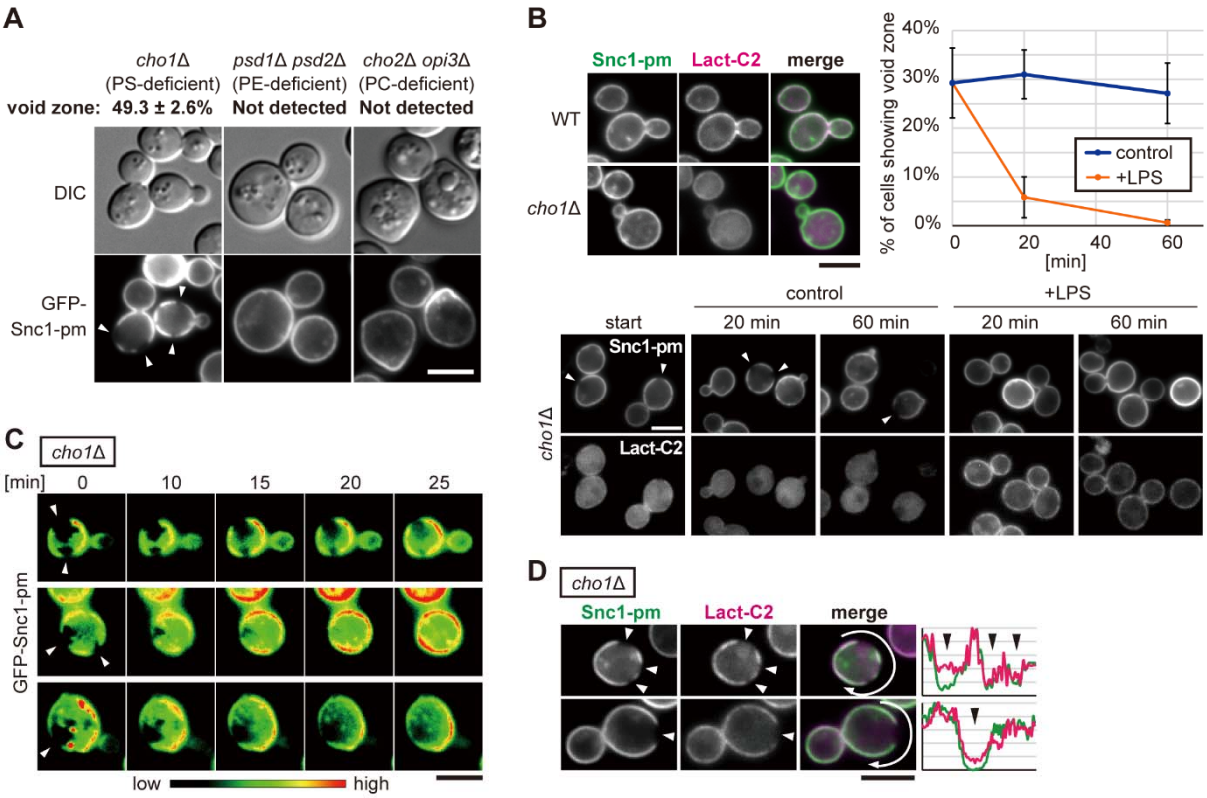

234

235 **Figure 3 Void zone formation is specific to PS depletion and is a reversible process.**

236 (A) The generation of the void zone is specific to the PS-deficient cells. All strains expressing
237 GFP-Snc1-pm were grown at 37°C. *cho1*Δ cells were grown in SD medium containing 1 mM
238 ethanolamine. *psd1*Δ *psd2*Δ cells were grown in SD medium containing 2 mM choline. *cho2*Δ
239 *opi3*Δ cells were grown in SD medium. Percentage of the cells with the void zone is indicated
240 as the mean and SD (n > 100 cells, three independent experiments). Arrowheads indicate the
241 void zone. Scale bar: 5 μm. (B) Regeneration of PS by lyso-PS supplementation dissipates the
242 void zone. Wild-type and *cho1*Δ cells expressing GFP-Snc1-pm and mRFP-Lact-C2 are
243 shown in the upper left panel. *cho1*Δ cells were grown in YPDA medium at 37°C in the
244 presence or absence of lyso-PS (20 μM). Percentage of the cells with the void zone was
245 examined at 20 and 60 min and shown as the mean and SD (n > 100 cells, three independent
246 experiments) (upper right panel). Representative images are shown in the lower panel.
247 Arrowheads indicate the void zone. Scale bars: 5 μm. (C) Time-lapse imaging of the void

zone disappearance induced by lyso-PS addition. *cho1*Δ cells expressing GFP-Snc1-pm were prepared as in (B). Cell suspension was placed on the agarose gel pad immediately after mixing with lyso-PS and time-lapse imaging was started. Three examples are shown in the pseudo-colour. Arrowheads indicate the void zone. Scale bar: 5 μm. (D) Void zones are not rapidly dissipated by PS. *cho1*Δ cells expressing GFP-Snc1-pm and mRFP-Lact-C2 were prepared as in (B). Images 20 min after supplementation with lyso-PS are shown. Fluorescence intensities of GFP and mRFP in the cell periphery (arrows) are plotted on the right. Arrowheads indicate the void zone. Scale bar: 5 μm.

Void zone restricts lateral diffusion of the inner leaflet-anchored proteins, but has no effect on a GPI-anchored protein.

We next examined whether the plasma membrane-localized peripheral membrane proteins can be distributed in the void zone. Three types of proteins were tested (Figure 4A). Ras2 is a small GTPase with the C-terminal lipid moiety inserted into the cytoplasmic leaflet of the plasma membrane. Ras2 undergoes farnesylation and palmitoylation, and the latter is required for membrane localization (Bhattacharya *et al.,* 1995). Gap1C is the C-terminal cytosolic region of the amino acid permease Gap1. Gap1 localizes to the plasma membrane, and Gap1C without the transmembrane domain is also localized at the plasma membrane (Popov-Čeleketić *et al.,* 2016). Gap1C is palmitoylated; however, its membrane localization is due to its amphipathic helix structure and not to the palmitoyl anchor (Popov-Čeleketić *et al.,* 2016). Gas1 is a cell wall protein with glycosylphosphatidylinositol (GPI)-anchor inserted into the extracellular leaflet of the plasma membrane (Nuoffer *et al.,* 1991). All these proteins were mainly localized to the plasma membrane in the wild-type cells (Figure 4B). In *cho1*Δ cells harbouring the void zone, Ras2 and Gap1C were absent from the void zone similar to Snc1-pm (Figure 4B). In contrast, Gas1 was uniformly distributed in the plasma membrane

regardless of the void zone (Figure 4B). These results suggest that the void zone restricts the lateral diffusion of the inner leaflet-associated proteins and the transmembrane proteins but does not influence the diffusion of proteins anchored to the outer leaflet. Normally, PS is abundantly distributed in the inner leaflet of the plasma membrane. These results suggest that formation of the void zone is mainly due to lipid changes in the inner leaflet rather than that in the outer leaflet.

Figure 4

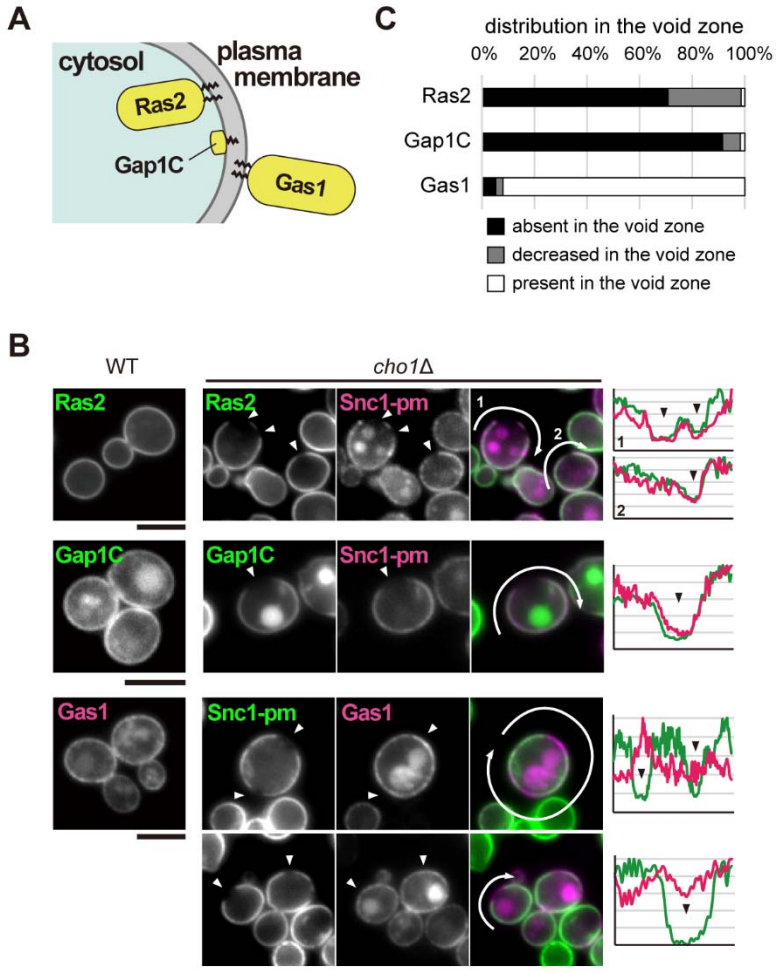

Figure 4 Distribution of peripheral membrane proteins in the void zone.

(A) Localization of three peripheral membrane proteins. (B) Ras2 and Gap1C were excluded from the void zone, but Gas1, a GPI-AP, was not excluded. Cells expressing GFP-Ras2 under

the control of the *GAL1* promoter and mRFP-Snc1-pm were grown in YPGA at 37°C. Cells expressing GFP-Gap1C and mRFP-Snc1-pm or GFP-Snc1-pm and mRFP-Gas1 were grown in SDA-U medium containing 1 mM ethanolamine at 37°C. Fluorescence intensities of GFP and mRFP in the cell periphery (arrows) are plotted on the right. Arrowheads indicate the void zone. Scale bars: 5 μm. (C) Cells observed as in (B) are categorized by the distribution of each protein in the void zones detected by Snc1-pm (n > 50 cells with the void zone).

Void zone is a liquid-ordered-like domain that requires ergosterol and sphingolipid for its formation.

Based on the fact that transmembrane proteins are excluded from the void zone, we hypothesized that the void zone is a liquid-ordered (Lo) domain formed by phase separation. When phase separation occurs in an artificial membrane containing saturated phospholipids (e.g., dipalmitoylphosphatidylcholine (DPPC) and sphingolipids), unsaturated phospholipids (e.g., dioleoylphosphatidylcholine (DOPC)), and cholesterol, cholesterol and saturated phospholipids form the Lo domains and unsaturated lipids are separated into the liquid-disordered (Ld) domains (Baumgart *et al.,* 2003; Baumgart *et al.,* 2007; Risselada and Marrink, 2008; Lingwood and Simons, 2010). Cholesterol preferentially interacts with lipids containing saturated acyl chains. Relative difference between affinities of cholesterol for unsaturated versus saturated phospholipids was suggested as one of the causes of phase separation (Engberg *et al.,* 2016). Importantly, molecular dynamics computer simulation, the giant unilamellar vesicle (GUV) assay, and giant plasma membrane vesicle (GPMV) assay have shown that transmembrane helices and transmembrane proteins are excluded from the Lo domains and segregated into the Ld domains (Sengupta *et al.,* 2008; Schäfer *et al.,* 2011). In addition, phase separation into the Lo and Ld phases occurs with yeast lipids in GUVs (Klose *et al.,* 2010). Therefore, we examined whether the void zone is a sterol-enriched lipid

domain. To assess the distribution of ergosterol, a major sterol in yeast, cells were stained with the sterol-binding dye filipin. Filipin showed a punctate distribution in the plasma membrane of the wild-type cells as reported previously (Grossmann *et al.,* 2007), whereas in *cho1*Δ cells, filipin mainly accumulated at the void zones (Figure 5A), indicating that the void zone is rich in ergosterol.

Similar to sterols, sphingolipids are important for the formation of the Lo domains (Dietrich *et al.,* 2001; Baumgart *et al.,* 2003; de Almeida *et al.,* 2003; Veatch and Keller, 2003). We therefore examined whether the biosynthesis of ergosterol and sphingolipid is required for the formation of the void zone. Erg2, Erg3, and Erg4 are essential enzymes for the synthesis of ergosterol (Silve *et al.,* 1996; Arthington *et al.,* 1991; Lai *et al.,* 1994). Ipt1 is an inositolphosphotransferase required for the synthesis of mannosyl-diinositolphosphorylceramide (M(IP)2C), the most abundant sphingolipid in yeast (Dickson *et al.,* 1997). Elo2 and Elo3, fatty acid elongases, participate in the long chain fatty acid biosynthesis of sphingolipids (Oh *et al.,* 1997). Sur2 and Scs7 are hydroxylases involved in the hydroxylation of sphingolipids (Haak *et al.,* 1997). Disruption of any of these genes essentially abolished the formation of the void zone (Figure 5B). Consistently, an inhibitor of ergosterol synthesis, fluconazole, blocked the formation of the void zone (Figure 5C). These results indicate that ergosterol and sphingolipids are necessary for the formation of the void zone and suggest that the void zone may be a Lo-like domain composed of abundant ergosterol and sphingolipids.

We further investigated whether the formation of the void zone results from an increase in the ergosterol level. The ergosterol level was increased in the *cho1*Δ cells grown at 37°C compared to that in the wild-type cells grown at 30°C. However, a similar increase in the ergosterol level was observed in the wild-type cells grown at 37°C and *cho1*Δ cells grown at

334 30°C, in which the void zone was not formed (Figure 5D). Therefore, the generation of the
335 void zone is not closely correlated with an increase in ergosterol.
336 The finding that the void zone is an ergosterol-rich lipid domain prompted us to investigate
337 the distribution of other lipids that can be visualized using the corresponding probes. To
338 examine the distribution of phosphatidylinositol 4-phosphate (PI(4)P), phosphatidylinositol
339 4,5-bisphosphate (PI(4,5)P2), and phosphatidic acid (PA), the PH domains of yeast Osh2 and
340 human PLCδ and the PA-binding domain of yeast Spo20 were used as the probes,
341 respectively (Roy and Levine, 2004; Lemmon *et al.,* 1995; Watt *et al.,* 2002; Nakanishi *et al.,*
342 2004). These probes were uniformly distributed in the plasma membrane in the wild-type
343 cells; however, none of the probes were detected in the void zone (Figure 5E). This result
344 suggests that PI(4)P, PI(4,5)P2, and PA cannot enter the void zone by lateral diffusion. The
345 majority of yeast phospholipids have mono- or di-unsaturated fatty acids (Schneiter *et al.,*
346 1999; Ejsing *et al.,* 2009; Klose *et al.,* 2012); hence, these results support the possibility that
347 the void zone corresponds with the Lo-domains.
348 We conclude that the void zone is a lipid domain with an unusual assembly of ergosterol that
349 cooperates with sphingolipids and thereby has Lo domain-like properties with limited lateral
350 diffusion of the peripheral membrane proteins and certain types of glycerophospholipids.
351

352 **Figure 5**

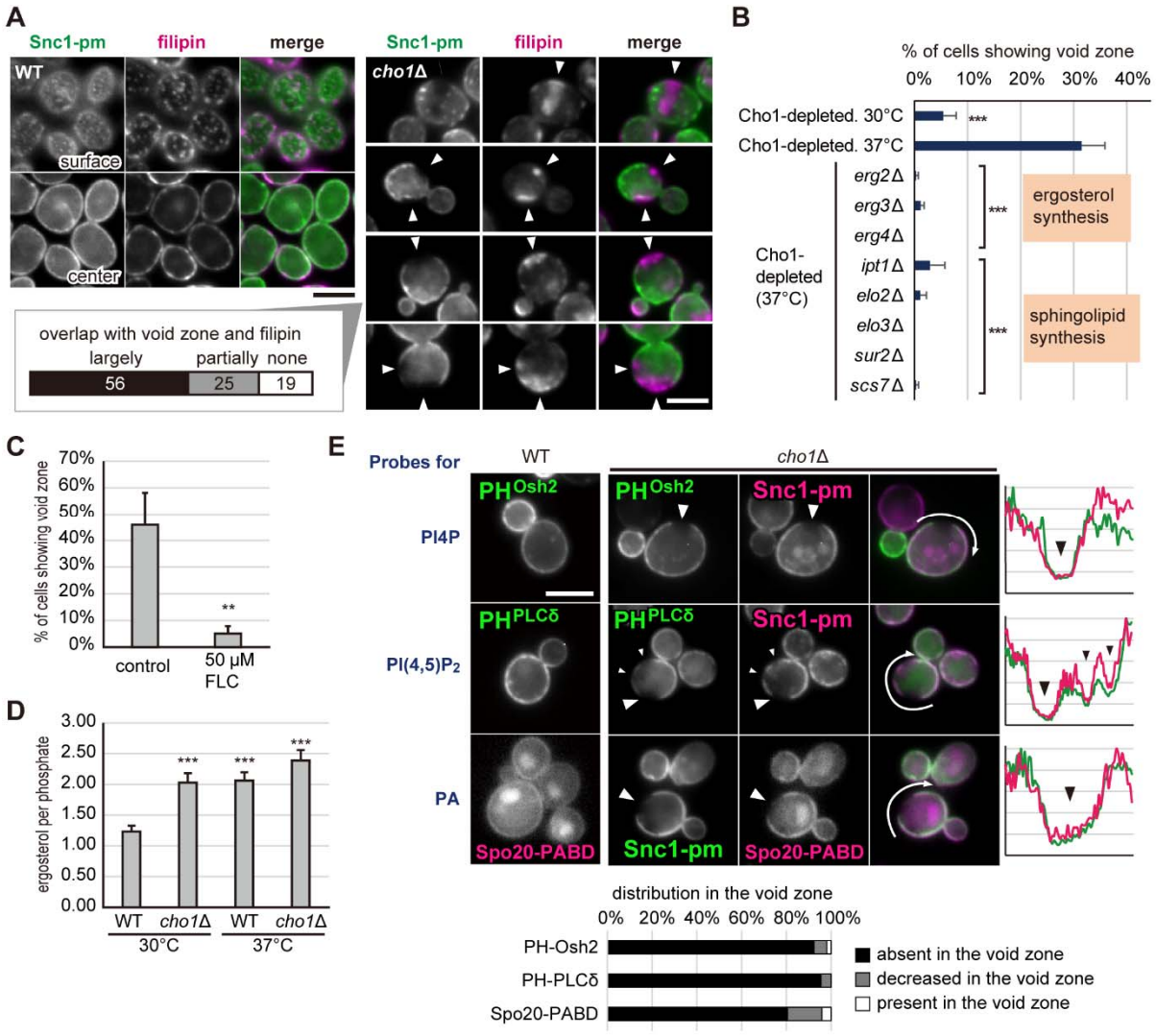

353

354 **Figure 5 Ergosterol is accumulated in the void zone.**

355 (A) Ergosterol accumulation in the void zone. Cells expressing GFP-Snc1-pm were grown in
356 YPDA medium at 37°C, fixed, and stained with filipin. The filipin staining patterns of *cho1*Δ
357 cells containing the void zone (n = 100) were categorized and are shown in the lower left
358 panel. Arrowheads indicate the void zone. Scale bars: 5 μm. (B) The formation of the void
359 zone was dependent on ergosterol and sphingolipids. Cells expressing GFP-Snc1-pm were
360 grown overnight in YPDA medium at the indicated temperature. The incidence of the void
361 zone (n > 100 cells) was examined in three independent experiments, and the data are shown
362 as the mean and SD. Asterisks indicate significant differences from the Cho1-depleted cells

grown at 37°C according to the Tukey–Kramer test (***, $p < 0.001$). (C) The void zone was not generated after ergosterol depletion by fluconazole. *cho1*Δ cells expressing GFP-Snc1-pm were precultured in YPDA medium at 30°C and incubated at 37°C for 6 h with or without 50 μM fluconazole. The incidence of the void zone ($n > 100$ cells) was examined and the data are shown as in (B). Asterisks indicate a significant difference according to the Student's t-test (**, $p < 0.005$). (D) The total levels of ergosterol in the wild-type and *cho1*Δ cells. Cells were grown overnight in YPDA medium at 30°C or 37°C, and total cellular lipids were extracted. Ergosterol contents were analysed by TLC. The ratio of total ergosterol to total phosphate (mol/mol) is shown as the mean and SD of four independent experiments. Asterisks indicate significant differences according to the Tukey–Kramer test (***, $p < 0.001$ compared to the wild-type at 30°C). (E) PIPs and PA were excluded from the void zone. Cells expressing mRFP-Snc1-pm and either Osh2-2xPH-3xGFP or GFP-PLCδ-2XPH were grown and observed as in (B). Cells expressing GFP-Snc1-pm and mCherry-Spo20-PABD were grown in SDA-U medium containing 1 mM ethanolamine at 37°C. Fluorescence intensities of GFP and either mRFP or mCherry around the cells (arrows) are plotted on the right. Arrowheads indicate the void zone. Scale bar: 5 μm. The distribution of each probe in the void zones detected by Snc1-pm ($n > 50$ cells with the void zone) is shown in the lower panel.

Vacuole, a lysosome-like organelle in yeast, contacts the void zone

Observations using the lipid probes suggest phase separation in the plasma membrane; the lipid composition of the void zone is different from that in the other plasma membrane regions. The plasma membrane and the ER form the membrane contact sites (MCSs) via ER-resident tethering proteins that interact with phospholipids of the plasma membrane (Saheki and De Camilli, 2017). To test whether the void zone can influence this ER-PM contact, we examined two ER marker proteins, Hmg1 and Rtn1 (Koning *et al.*, 1996; De Craene *et al.*,

2006). The cortical ER (cER) was clearly absent at the void zone in the *cho1*Δ cells (Figure 6A; 89.2% of Hmg1, 92.9% of Rtn1, n > 100 cells, respectively). The ER-PM tethering proteins Tcb1/2/3, and Ist2 were reported to bind to PS and PI(4,5)P2, respectively (Schulz and Creutz, 2004; Fischer *et al.,* 2009). Since PS is not synthesized in the *cho1*Δ cells and PI(4,5)P2 is not distributed in the void zone (Figure 5E), the association of cER with the plasma membrane may be lost in the void zone.

To investigate whether the void zone influences the distribution or morphology of other organelles, several organelle markers were examined in the *cho1*Δ cells. Surprisingly, we found that vacuoles were in contact with the void zones (Figure 6B). The observations using Snc1-pm and FM4-64 indicate that the contact between the void zone and the vacuole was detected in 45.1% of the *cho1*Δ cells with the void zone (45.1 ± 7.0%, five independent experiments, n > 50 cells each). The proximity of the non-void zone regions and vacuoles was observed only in 7.8% of the *cho1*Δ cells (7.8 ± 1.7%, three independent experiments, n > 100 cells each) compared to that in the wild-type cells (10.1 ± 2.1%, three independent experiments, n > 100 cells each). These data suggest that frequent contact of the vacuoles with the plasma membrane is specific to the void zone. The fact that not all void zones are in contact with the vacuoles indicates that the exclusion of the transmembrane proteins from the void zones was not caused by the vacuole contact (Figure 6B). On the other hand, the *trans*-Golgi network (TGN), lipid droplets, and mitochondria did not contact the void zone (Figure 6—figure supplement 1), suggesting that only vacuoles interact with the void zone. This type of contact between the plasma membrane and the vacuoles or lysosomes has not been reported, and we refer to the contact between the void zone and vacuoles as the "V-V contact".

In stationary phase yeast cells, a raft-like domain is formed in the vacuolar membrane, where lipophagy, the uptake of the lipid droplets, occurs (Toulmay and Prinz, 2013; Wang *et al.,*

2014; Tsuji *et al.,* 2017). The properties of this vacuolar microdomain are very similar to the properties of the void zone, including absence of the transmembrane proteins and ergosterol enrichment. To test whether this vacuolar microdomain is present in the void zone contact area, we examined three vacuolar transmembrane proteins, Vph1, Cot1, and Zrc1 (Manolson *et al.,* 1992; Li and Kaplan, 1998). These proteins were uniformly distributed in the vacuolar membrane of the wild-type cells; however, in some vacuoles in contact with the void zone of the *cho1*Δ cells, these proteins were excluded from the contact area (Figure 6C). One of these proteins, Vph1, had the highest frequency of segregation on vacuoles in contact with the void zone (73.5% of Vph1, 41.5% of Cot1, and 30.0% of Zrc1, $n > 50$). In contrast, the exclusion of FM4-64 dye in vacuoles of the cells with the V-V contacts was not detected ($n > 50$; Figure 6B). These data suggest that certain vacuoles form a membrane domain at the V-V contact site.

To understand the dynamics of the V-V contact, we used time-lapse imaging with GFP-Snc1-pm and Vph1-mRFP (Video 1) and detected two patterns. First, the movement of a vacuole into the void zone was observed (Figure 6D, shown as "a"). The speed of the vacuole migration to the void zone was highly variable between individual cells. However, some void zones had no contact with the vacuoles during the 1 h observation. Second, the V-V contact lasted over half an hour (Figure 6D, shown as "b"). In one hour of observation of the cells with the void zone, 60% of the cells had the V-V contact over 30 min (Figure 6E). The disappearance of the void zone after its formation was rarely observed, and this phenomenon appears to be unrelated to the presence or absence of the V-V contacts. In addition, no vacuoles left the void zone while the void zone was maintained. The molecular basis of the V-V contact is unknown although this contact appears to be stable. Vacuoles in contact with the void zone underwent fission and fusion (Figure 6—figure supplement 2).

438 **Figure 6**

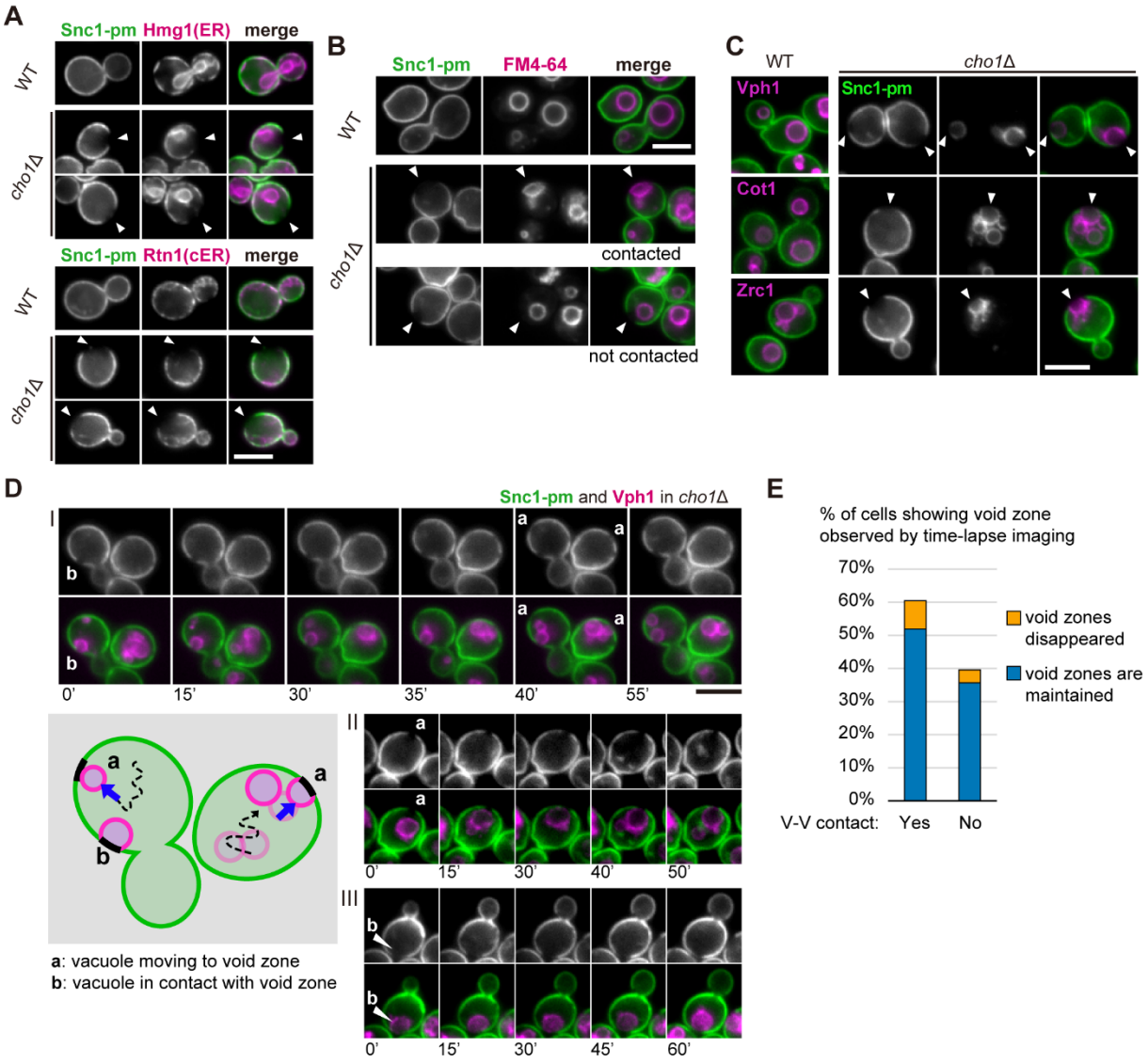

439

440 **Figure 6 Vacuoles contact the void zone.**

441 (A) Cortical ER is disassociated from the void zone. Cells expressing mRFP-Snc1-pm and
442 either Hmg1-GFP or Rtn1-GFP were grown in YPDA medium at 37°C. The mRFP-Snc1-pm
443 and ER marker proteins are shown in green and magenta, respectively. Arrowheads indicate
444 the void zone. Scale bar: 5 μm. (B) Vacuoles contact the void zone. Cells expressing GFP-
445 Snc1-pm were grown in YPDA medium at 37°C and stained with FM4-64 for 20 min.
446 Arrowheads indicate the void zone. Scale bar: 5 μm. (C) Separation of the vacuolar protein in
447 the void zone contact region. Cells expressing mRFP-Snc1-pm and either Vph1-GFP or GFP-

448 Cot1 and cells expressing GFP-Snc1-pm and mRFP-Zrc1 were grown in YPDA medium at
449 37°C. Snc1-pm and vacuolar proteins are shown in green and magenta, respectively.
450 Arrowheads indicate the void zone. Scale bar: 5 μm. (D) Time-lapse imaging of the vacuole-
451 void zone contact. *cho1*Δ cells expressing GFP-Snc1-pm and Vph1-mRFP were grown in
452 YPDA medium at 37°C. Three examples with two distinctive patterns (a, b) are shown. In the
453 bottom left scheme, black regions in the plasma membrane indicate the void zone. Numbers
454 indicate time in min. Scale bar: 5 μm. (E) The vacuole-void zone contact is stable. Cells
455 observed by time-lapse imaging as in (D) are categorized by the presence or absence of the V-
456 V contact and the void zone behaviour (n > 100 cells with the void zone). Estimation was
457 based on the void zone or the V-V contact lasting more than 30 min during 1 h observation.
458

459 **Figure 6 S1**

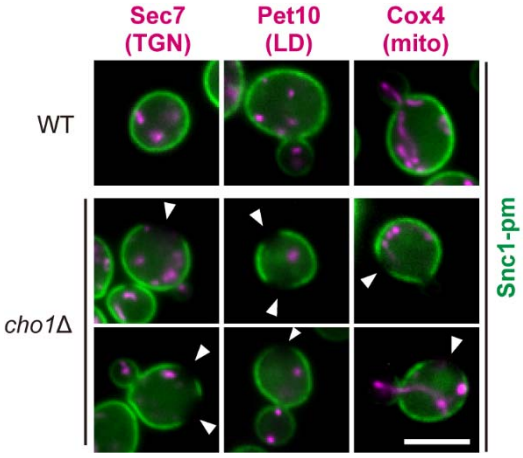

460

461 **Figure 6-Figure supplement 1 Distribution of organelles in the cells with the void zone.**
462 The distribution of the *trans*-Golgi network (TGN), lipid droplets (LD), and mitochondria
463 (mito) is not influenced by the void zone. Cells expressing GFP-Snc1-pm and Sec7-mRFP,
464 Pet10-GFP and mRFP-Snc1-pm, or Cox4-GFP and mRFP-Snc1-pm were grown in YPDA or
465 SDA-U media at 37°C. Snc1-pm and the organelle marker proteins are shown in green and
466 magenta, respectively. Arrowheads indicate the void zone. Scale bar: 5 μm.
467

468 **Figure 6 S2**

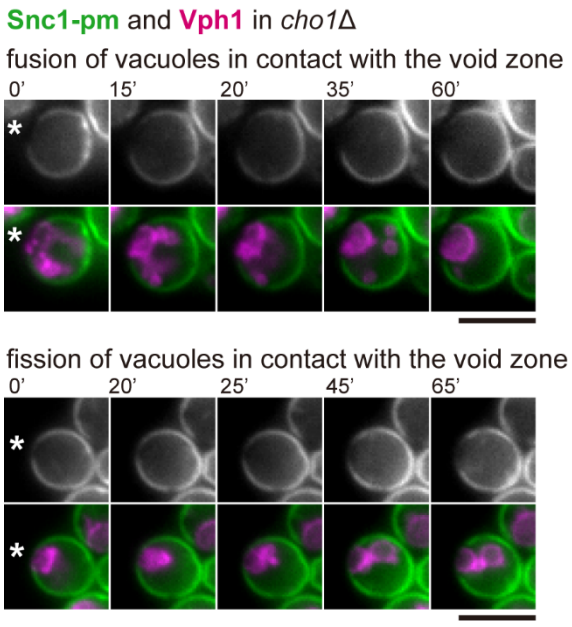

469

470 **Figure 6-Figure supplement 2 Fusion and fission of vacuoles in contact with the void**

471 **zone.**

472 Time-lapse imaging of the vacuole-void zone contact was performed. *cho1*Δ cells expressing

473 GFP-Snc1-pm and Vph1-mRFP were grown in YPDA medium at 37°C. Fusion and fission of

474 vacuoles in contact with the void zone are shown in the upper and lower panels, respectively.

475 Numbers indicate time in min. Asterisks indicate the V-V contact. Scale bars: 5 μm.

476

Video 1 (thumbnail image)

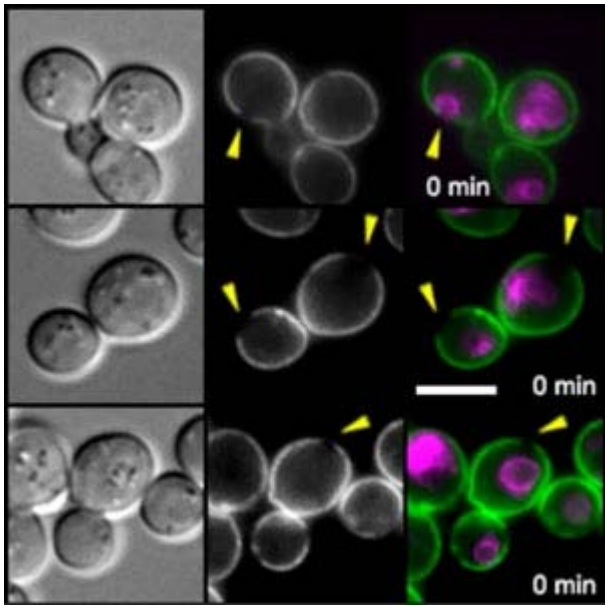

Video 1

Time-lapse imaging of the vacuole-void zone contact. Time-lapse imaging was performed as in Figure 6D and Materials and Methods. Three samples are shown. Yellow arrowheads indicate the void zone. Yellow circles indicate the V-V contact site. Scale bar: 5 μm.

Identification of the genes required for the formation of the void zone

To further understand the mechanism of the void zone formation, we created a series of deletion mutants on the background of the *cho1*Δ or glucose-repressible P_{GAL1}-*3HA-CHO1* mutations and examined their effect on the generation of the void zone (Figure 7A). Various genes involved in sterol trafficking were tested, and the results indicate that *kes1*Δ (*osh4*Δ) mildly and *arv1*Δ significantly reduced the void zone formation. Kes1 is one of the yeast oxysterol-binding proteins that exchanges sterols for PI(4)P between the lipid membranes (Jiang, *et al.*, 1994; de Saint-Jean *et al.*, 2011). Arv1 was implicated in the GPI-anchor biosynthesis and transport and in intracellular sterol distribution (Kajiwara *et al.*, 2008; Beh and Rine, 2004). Both Kes1 and Arv1 are involved in the sterol transport; however, their contribution to the sterol transport to the plasma membrane is very low (Georgiev *et al.*, 2011;

Georgiev *et al.,* 2013). These proteins regulate sterol organization in the plasma membrane; the mutations influence the sensitivity to the sterol-binding drugs and sterol-extraction efficiency of MβCD (Georgiev *et al.,* 2011; Georgiev *et al.,* 2013). These differences in sterol organization may influence the formation of the void zone. Npc2 is an orthologue of Niemann-Pick type C protein and plays an essential role together with Ncr1 in sterol insertion into the vacuolar membrane from the inside of the vacuole, which is required for the formation of the raft-like vacuolar domain during lipophagy in the stationary phase (Tsuji *et al.,* 2017). However, deletion of Npc2 did not influence generation of the void zone or formation of the V-V contacts accompanied with protein-free vacuolar domain (Figure 7—figure supplement 1A). This result suggests that the void zone is formed independently of Ncr1/Npc2-mediated sterol transport possibly because Ncr1/Npc2 are not involved in sterol organization in the plasma membrane. The vacuolar domains detected at the V-V contact region and generated during the stationary phase lipophagy are similar in appearance; however, the processes of their formation may be different.

The void zone formation was observed in the absence of Pep4, a major vacuolar protease, and Vac17, a myosin adapter required for inheritance of vacuoles. However, the void zone formation was strongly suppressed by deletion of Vma2 and Fab1.

Vma2 is a subunit of the V-ATPase that regulates pH homeostasis and functions as a pH sensor (Marshansky *et al.,* 2014). Consistent with this observation, other genes involved in pH homeostasis (*NHA1*, *NHX1*, *RIM21*, and *RIM101*) were required for the void zone formation (Figure 7A, pH regulation) (Sychrová *et al.,* 1999; Brett *et al.,* 2005; Obara *et al.,* 2012). Thus, we examined the effect of pH of the medium on the formation of the void zone. The formation of the void zone was strongly suppressed by increasing pH in the medium from 6.6 to 7.5. (Figure 7B). On the other hand, the low pH medium (pH 4.0) slightly increased the formation of the void zone. Interestingly, the frequency of the V-V contacts was significantly

520 reduced in the low pH medium (Figure 7C). The mechanism of these pH-dependent
521 phenomena is unclear although they may be important in assessment of the molecular basis of
522 the formation of the void zones and V-V contacts.
523 Fab1 is a phosphatidylinositol 3-phosphate (PI(3)P) 5-kinase that generates
524 phosphatidylinositol 3,5-bisphosphate (PI(3,5)P2) (Cooke *et al.,* 1998). PI(3,5)P2 functions as
525 a signal lipid in intracellular homeostasis, adaptation, and retrograde membrane trafficking
526 (Jin *et al.,* 2016). We speculated that the defects in the retrograde transport may indirectly
527 influence the void zone formation in the plasma membrane and thus examined various genes
528 involved in the membrane transport. Strikingly, conserved protein complexes, retromer, class
529 C core vacuole/endosome tethering (CORVET), homotypic fusion and vacuole protein sorting
530 (HOPS), and endosomal sorting complexes required for transport (ESCRT) were required for
531 the void zone formation (Figure 7A and D). As the name implies, the Vps proteins belonging
532 to these complexes were identified using mutants defective in vacuolar protein sorting (VPS)
533 (Robinson *et al.,* 1988; Rothman *et al.,* 1989). Dysfunction of these complexes perturbs
534 intracellular vesicle trafficking (Schmidt and Teis, 2012; Balderhaar and Ungermann, 2013;
535 Burd and Cullen, 2014), which may influence the plasma membrane recycling of cargo and
536 lipids involved in the void zone formation. Similarly, proteins involved in the retrograde
537 transport, such as the SNAREs Pep12 and Tlg2, the epsin-like adapter Ent3/Ent5, and the
538 clathrin adapter Gga1/Gga2, were required for the void zone formation. A dynamin-like
539 GTPase Vps1, Arf-like GTPase Arl1, and Rab6 GTPase homologue Ypt6 are known to be
540 closely related to the membrane trafficking (Vater *et al.,* 1992; Li and Warner, 1996;
541 Rosenwald *et al.,* 2002). Consistent with this notion, *vps1*Δ, *arl1*Δ, and *ypt6*Δ inhibited the
542 void zone formation. Impaired membrane transport in the inner membrane system can be
543 manifested as the changes in the plasma membrane lipid organization and/or defects in the pH
544 control. However, Apl2 and Apl1, the subunits of the adaptor complexes AP-1 and AP-2,

545 respectively, had little contribution to the void zone formation presumably because these
546 mutants had insignificant disruption of the membrane trafficking compared to the effects of
547 *ent3*Δ, *ent5*Δ and *gga1*Δ *gga2*Δ (Yeung *et al.,* 1999; Sakane *et al.,* 2006; Morvan *et al.,*
548 2015). Deletion of *APL5*, which encodes the subunit of AP-3 responsible for the transport
549 from the Golgi to the vacuole (Dell'Angelica, 2009), slightly reduced the void zone formation,
550 suggesting the importance of the vacuolar functions for the void zone formation.
551 Deletion of the autophagy-related genes (*atg1*Δ, *atg10*Δ, *atg12*Δ, and *atg15*Δ) did not
552 influence the void zone formation. *ATG1* is one of the core ATG genes (Mizushima *et al.,*
553 2011). The void zone was generated and the V-V contact with the vacuolar microdomain was
554 observed in the absence of Atg1 (Figure 7A, and Figure 7—figure supplement 1B). This
555 result suggests that the void zone formation is independent of autophagy consistent with our
556 notion that direct or indirect effects on lipid organization in the plasma membrane (e.g., *via*
557 the Vps pathway) are influencing the void zone formation.
558 We also examined the effect of mutations in the flippase-related proteins. The deficiency of
559 Cdc50 or Any1/Cfs1 localized in endosomes and the TGN had little effect on the void zone
560 formation (Saito *et al.,* 2004; van Leeuwen *et al.,* 2016; Yamamoto *et al.,* 2017); however,
561 disruption of Lem3 localized in the plasma membrane completely suppressed the generation
562 of the void zone (Kato *et al.,* 2002). The Lem3-Dnf1/2 flippase complexes translocate
563 glycerophospholipids, but not ceramides and sphingolipids, to the cytoplasmic leaflet of the
564 lipid bilayer (Pomorski *et al.,* 2003; Saito *et al.,* 2004; Furuta *et al.,* 2007). We assumed that
565 disruption of the phospholipid asymmetry by *lem3*Δ may influence ergosterol behaviour in
566 the plasma membrane. To test this hypothesis, we examined the sensitivity to an antifungal
567 ergosterol-binding drug, amphotericin B (AmB) (Kamiński, 2014). The results indicate that
568 *lem3*Δ is highly sensitive to AmB, which is detected in the *cho1*Δ background cells, and this
569 effect was cancelled by addition of *erg6*Δ that causes defects in ergosterol biosynthesis

570 (Figure 7E). Thus, the disruption of phospholipid asymmetry alters the ergosterol distribution
571 in the plasma membrane, thereby suppressing the void zone formation (see discussion).

572

573 **Figure 7**

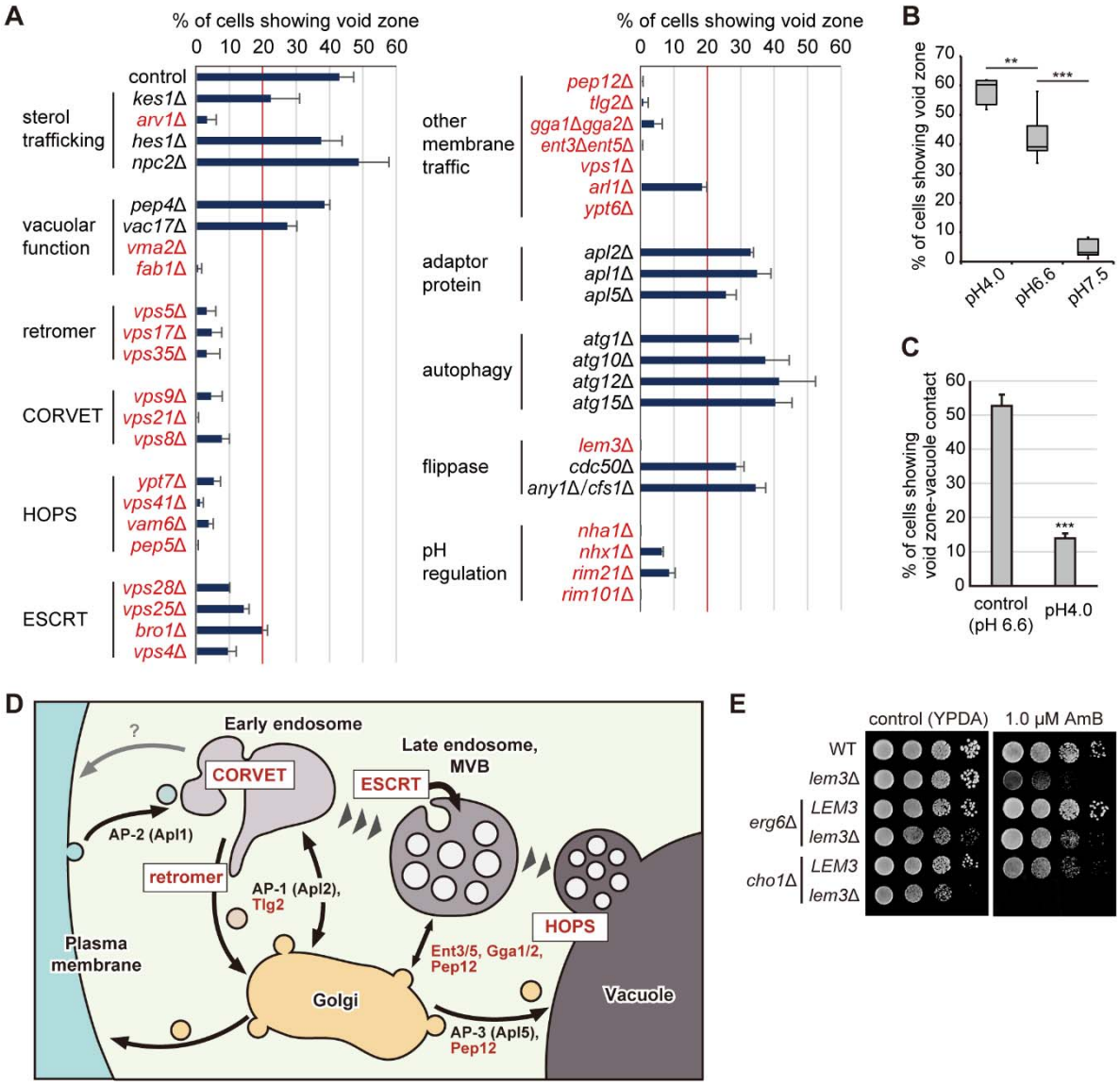

574

575 **Figure 7 A search for the genes required for the void zone formation**

576 (A) Frequency of the void zone in the mutant cells generated on *cho1*Δ background or under
577 Cho1-depleted conditions. The incidence of the void zone was determined (n > 100 cells,
578 three independent experiments) and is shown as the mean and SD. The mutations responsible
579 for the low incidence (under 20%) are shown in red. (B) The void zone formation is

suppressed by high pH. *cho1*Δ cells expressing GFP-Snc1-pm were grown overnight in YPDA at the indicated pH at 37°C. The incidence of the void zone was determined (n > 100 cells, five independent experiments) and is shown as a box plot. Asterisks indicate significant differences according to the Tukey–Kramer test (**, $p < 0.005$; ***, $p < 0.001$). (C) Low pH decreases the frequency of the V-V contact. *cho1*Δ cells expressing GFP-Snc1-pm and Vph1-mRFP were grown in YPDA at the indicated pH at 37°C. The incidence of the V-V contacts was determined (n > 100 cells with the void zone, three independent experiments) and is shown as the mean and SD. Asterisks indicate a significant difference according to the Student's t-test (***, $p < 0.001$). (D) A scheme of the membrane trafficking. Proteins and protein complexes required for the formation of the void zone are shown in red. (E) The loss of phospholipid asymmetry in the plasma membrane results in high sensitivity to amphotericin B. Serial dilutions of the cultures were spotted onto YPDA plates containing 1.0 μM amphotericin B and incubated at 30°C for 2 d.

Figure 7 S1

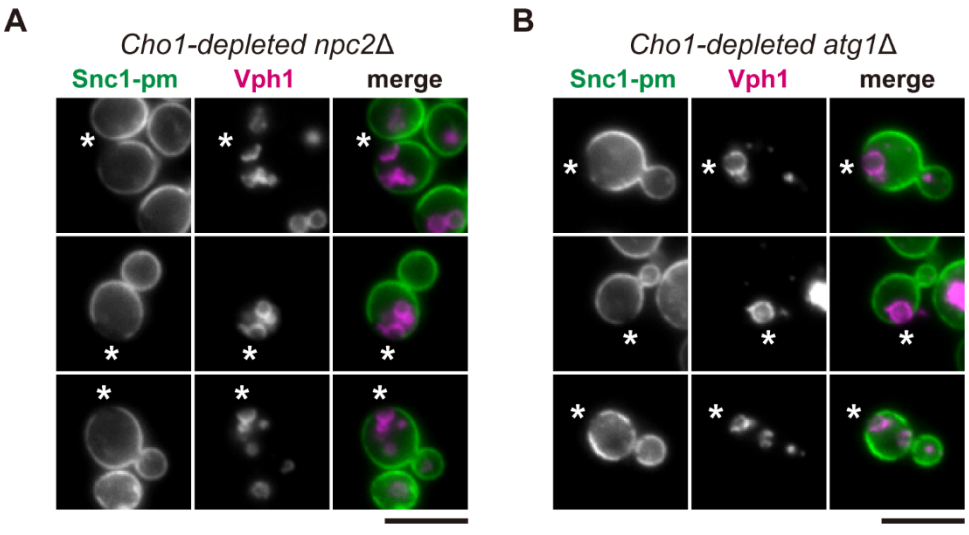

Figure 7-Figure supplement 1 Npc2 and Atg1 are not essential for the formation of the void zone and the V-V contacts.

598 (A and B) The void zone and the V-V contact in the absence of Npc2 and Atg1. Cells
599 expressing GFP-Snc1-pm and Vph1-mRFP were grown in YPDA medium at 37°C. Asterisks
600 indicate the V-V contact. Scale bars: 5 μm.
601

602 ## Discussion

603 In the artificial membranes, phase separation causes micron-scale separation of proteins and
604 lipids; such large separation does not occur in the plasma membrane of the living cells. The
605 mechanism that enables random distribution of proteins and lipids throughout the plasma
606 membranes on the macroscopic scale by preventing large-scale phase separation has not been
607 understood. We found that in PS-deficient cells grown at high temperatures, the protein-free
608 membrane domain "void zone" develops in the plasma membrane and exhibits Lo phase-like
609 properties (Figure 8). We propose a new role of PS in membrane organization and suggest
610 that PS prevents the occurrence of abnormal membrane domains due to phase separation and
611 ensures macroscopic homogeneity of the distribution of the molecules on the plasma
612 membrane.
613

614 **Mechanisms of the generation and disappearance of the void zone**

615 PS is a phospholipid mainly distributed in the inner leaflet of the plasma membrane and has a
616 relatively high affinity for cholesterol (Maekawa and Fairn, 2015; Nyholm *et al.,* 2019).
617 Therefore, loss of PS may alter relative affinity of the phospholipids for ergosterol in the inner
618 leaflet and may also influence the transbilayer distribution of ergosterol. Almost all yeast
619 phospholipids, including PS, have at least one unsaturated fatty acid; however, a small
620 fraction of phosphatidylinositol (PI) has only saturated fatty acids (Schneiter *et al.,* 1999;
621 Ejsing *et al.,* 2009; Klose *et al.,* 2012). Molecular species of PS, PE, PC, and PI were
622 characterized in the isolated plasma membrane; interestingly, 29.2% of PI have two saturated

623 fatty acids (Schneiter *et al.,* 1999). Relative affinity of ergosterol to various phospholipid
624 species is unclear. One hypothesis is that ergosterol is not clustered due to the interactions
625 with unsaturated PS in the wild-type cells; however, in *cho1*Δ cells, saturated PI becomes the
626 most dominant interaction partner of ergosterol in the inner leaflet of the plasma membrane
627 thus creating a driving force for phase separation. When PS is resynthesized in the *cho1*Δ
628 cells after the addition of lyso-PS, the void zone may disappear because PS becomes the
629 predominant interaction partner of ergosterol (Figure 3B and C).
630 Generation of the void zone requires PS deficiency and high temperature conditions. In
631 GUVs and GPMVs, lower temperature is favourable for phase separation, which occurs
632 within seconds (Dietrich *et al.,* 2001; Veatch and Keller, 2003; Baumgart *et al.,* 2007;
633 Levental I *et al.,* 2009). On the other hand, the development of the void zone requires
634 incubation for several hours at a high temperature (Figure 1B); thus, we speculate that the
635 remodelling of the lipid composition under high temperature may trigger the void zone
636 formation in the *cho1*Δ cells. In yeast, high temperature reduces the degree of unsaturation
637 and increases the acyl chain length of glycerophospholipids (Klose *et al.,* 2012), and these
638 events promote phase separation in the liposomes (Engberg *et al.,* 2016). A combination of
639 PS deficiency and high temperature-induced lipid remodelling may create a specific
640 membrane environment that results in the void zone development.
641 The void zones rapidly disappeared when the *cho1*Δ cells undergo a diauxic shift (Figure
642 2C) or when glucose or ATP is depleted from the medium (Figure 2D). During glucose
643 starvation, activities of the plasma membrane H^+-ATPase Pma1 and V-ATPase are reduced
644 (Young *et al.,* 2010; Dechant *et al.,* 2010). Therefore, the disappearance of the void zone may
645 be caused by a disturbance of pH homeostasis consistent with the suppression of the void
646 zone formation by mutations in the genes involved in pH homeostasis, including *VMA2*
647 (Figure 7A). Reduced activities of Pma1 and V-ATPases lead to acidification of the cytosol,

and the void zone formation is also inhibited in the medium with elevated pH (Figure 7B). The relationship between pH and phase separation is largely unknown; however, it has been reported that phase separation occurs at low pH and not at high pH in the artificial membranes that mimic human stratum corneum (Plasencia *et al.,* 2007).

Our results indicate that long chain fatty acids and hydroxylation of sphingolipids are necessary for the void zone formation (Figure 5B). It has been reported that GUVs prepared from the yeast total lipids have extensive phase separation, which depends on long fatty acid elongation and hydroxylation of sphingolipids (Klose *et al.,* 2010). M(IP)2C with a C26 fatty acid is the most common yeast sphingolipid species and its levels are significantly reduced in the *elo2*Δ and *elo3*Δ mutants (Oh *et al.,* 1997; Ejsing *et al.,* 2009). A recent study using asymmetric GUVs suggested that C24 SM and not C16 SM has a role in cholesterol retention in the inner leaflet of the lipid bilayer (Courtney *et al.,* 2018). Consistently, dehydroergosterol, a closely related fluorescent analogue of ergosterol, is mainly located in the inner leaflet of the plasma membrane, and this asymmetry is maintained by sphingolipids in yeast (Solanko *et al.,* 2018). This type of interaction of ergosterol with sphingolipids may be necessary for the void zone formation.

Ceramides may be another factor in the void zone formation in addition to PS, sterol, and sphingolipids. Ceramides form highly ordered domains in the model membranes; however, their interactions with cholesterol and phospholipids in the phase separation are very complex (Goñi and Alonso, 2009; López-Montero *et al.,* 2010; García-Arribas *et al.,* 2016). Yeast cells contain numerous long-chain ceramides in the plasma membrane (Schneiter *et al.,* 1999), and ceramide levels has been shown to increase at high temperature (Wells *et al.,* 1998; Klose *et al.,* 2012).

Analysis using several mutant strains on the *cho1* background revealed that retrograde intracellular trafficking has a significant effect on the void zone formation (Figure 7A).

673 Perturbed membrane transport may alter the distribution of the proteins and the key lipids as
674 described above. Moreover, *ARV1* and *LEM3* are important for the void zone formation. In
675 *arv1*Δ cells and Δtether cells that lack the ER-PM contacts, the transport of ergosterol to the
676 plasma membrane is essentially unchanged, whereas there were significant changes in
677 ergosterol accessibility to the compounds, such as increased efficiency of ergosterol
678 extraction with MβCD and increased sensitivity to the sterol-binding drug nystatin (Georgiev
679 *et al.* 2013; Quon *et al.,* 2018). Similarly, *lem3*Δ does not change the total ergosterol level
680 (Mioka *et al.,* 2018), and Dnf1 and Dnf2 do not contribute to the asymmetric distribution of
681 the ergosterol analogues across the plasma membrane bilayer (Solanko *et al.,* 2018).
682 However, *lem3*Δ cells are highly sensitive to AmB (Figure 7E). Thus, similar to the *arv1*Δ
683 and Δtether mutations, *lem3*Δ may alter the ergosterol distribution in the plasma membrane
684 thus preventing the formation of the void zone.
685
686 **The void zone has the exclusivity similar to Lo domains.**
687 Four observations support the notion that the void zone is a Lo phase-like domain: 1) absence
688 of the transmembrane proteins, 2) absence of certain peripheral membrane proteins, 3)
689 exclusion of certain types of glycerophospholipids, and 4) enrichment in sterols and the
690 contribution of sphingolipids.
691 We confirmed that the transmembrane proteins were completely excluded from the void
692 zone by the freeze-fracture replica labelling (Figure 1G and H). Similar segregation of the
693 transmembrane proteins has been observed in the Lo domains in computer simulations,
694 GUVs, and GPMVs (Baumgart *et al.,* 2007; Sengupta *et al.,* 2008; Kaiser *et al.,* 2009; Schäfer
695 *et al.,* 2011); however, this is the first report on a large and stable separation detected in the
696 plasma membrane of the living cells.

We also found that the lipid-anchored Ras2 cannot enter the void zone (Figure 4B). In the phase-separated artificial membranes, similar lipid-anchored peripheral proteins are also excluded from the Lo domains and separated into the Ld domains (Baumgart *et al.,* 2007; Sengupta *et al.,* 2008). In addition, the C-terminal region of Gap1 (Gap1C), which has an amphipathic helix, avoided the void zone (Figure 4B). In the artificial membranes, GTP-bound Arf1 can bind lipid membranes of variable curvature and lipid composition via its N-terminal amphipathic helix; however, Arf1 does not bind to the Lo domains (Krauss *et al.,* 2008; Manneville *et al.,* 2008; Giménez-Andrés *et al.,* 2018). In the case of Ras2 and Gap1C, the void zone properties were similar to those of the Lo domains in the artificial membranes. However, a GPI-anchored protein (GPI-AP), Gas1, does not have any significant separation in the void zone (Figure 4B), whereas mammalian GPI-AP has been reported to prefer the Lo domains in GPMVs (Baumgart *et al.,* 2007; Sengupta *et al.,* 2008). This discrepancy may be due to the differences in the nature of GPI-APs in yeast versus mammals (Pittet and Conzelmann, 2007; Fujita and Kinoshita, 2012; Muñiz and Zurzolo, 2014): 1) the plasma membrane-localized GPI-APs in yeast closely interact with the cell wall; 2) the fatty acid length of the GPI-anchor differs between yeast and mammals; 3) the nanodomains of GPI-APs have been visualized in mammalian cells (Sharma *et al.,* 2004) but have not been reported in yeast.

In addition to proteins, lipid probes suggest the separation of the phospholipids, PI(4)P, PI(4,5)P2, and PA, from the void zone (Figure 5E). The majority of the yeast phospholipids have mono- or di-unsaturated fatty acids (Schneiter *et al.,* 1999; Ejsing *et al.,* 2009; Klose *et al.,* 2012), and the unsaturated phospholipids, such as dioleoylphosphatidylethanolamine (DOPE), are separated from the Lo domains in the artificial membranes (Baumgart *et al.,* 2007; Sengupta *et al.,* 2008; Kaiser *et al.,* 2009). Therefore, absence of the lipid probes in the void zone is consistent with our notion that the void zone is a Lo-like domain. If the void zone

722 would have been composed of the PI species with saturated fatty acids as described above,
723 yeast PI kinases might have preferred the PI species with unsaturated fatty acids as the
724 substrates.
725
726 **Membrane contact between the void zone and vacuoles**
727 We have detected the contact between the void zone and the vacuoles (Figure 6B and D,
728 Figure 8A), and the time-lapse imaging revealed that this contact lasted for at least 30 min in
729 most cases (Figure 6D and E). These results suggest that the contact vacuoles may not
730 contribute to the rapid degradation and disappearance of the void zone. The contact vacuoles
731 are more likely to play a role in sealing the void zone to protect the cells. Recent studies
732 reported that in the phase-separated membranes with the Ld and Lo domains, membrane
733 permeability is increased at the interface between the two domains (Cordeiro, 2018). A
734 similar result indicated that the ER-PM contact sites are important for the maintenance of the
735 integrity of the plasma membrane (Omnus *et al.,* 2016; Collado *et al.,* 2019). In this study, we
736 found that void zone has Lo phase-like properties and that cortical ER is dissociated from the
737 void zone. Therefore, it is possible that the void zone induces high local permeability and low
738 integrity; thus, the void zone may be a fragile region of the plasma membrane. The V-V
739 contact may represent a protective cellular response to these plasma membrane abnormalities.
740 Our results also suggest that membrane domains may be formed on the vacuolar
741 membranes in contact with the void zone (Figure 6C). A contact between the membrane
742 domains accompanied by protein separation has been detected in the nucleus-vacuole junction
743 (NVJ), which is one of the MCSs that excludes certain proteins from the nuclear and vacuolar
744 membranes (Pan *et al.,* 2000; Dawaliby and Mayer, 2010; Toulmay and Prinz, 2013). The
745 transmembrane proteins appear to be completely excluded from the void zone (Figure 1H);

746 hence, the lipid-protein interactions via protein tethering may be present in the V-V contact
747 similar to that detected in the ER-PM contact sites.

748

749 **Figure 8**

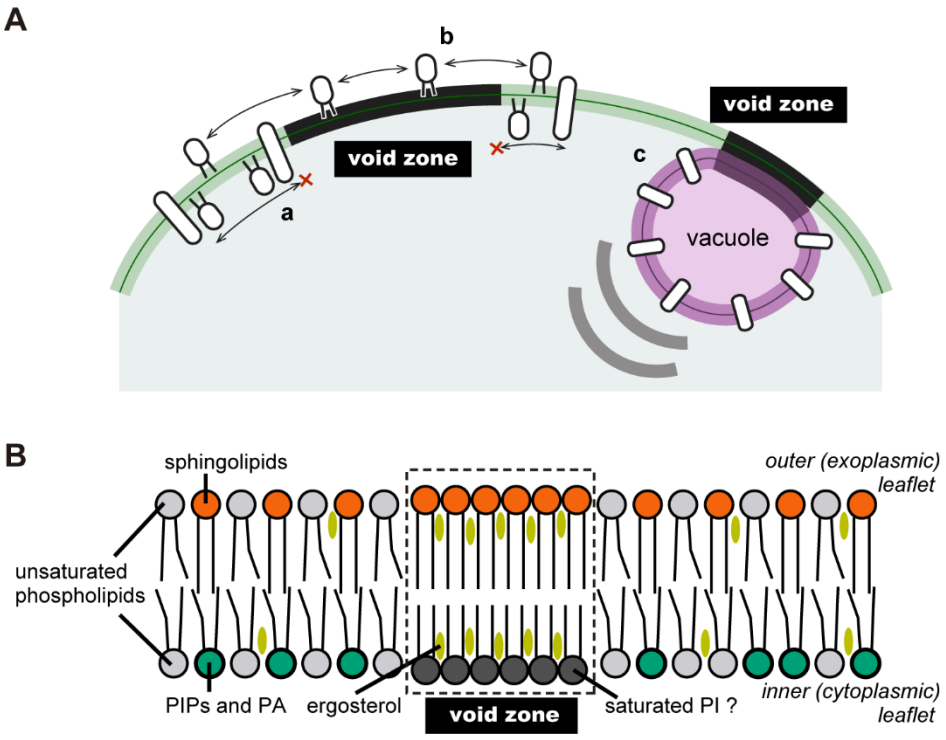

750

751 **Figure 8 Summary and a model of the void zone**

752 (A) Characteristics of the void zone revealed in this study. Our results suggest the following
753 properties of the void zone: (a) transmembrane proteins and peripheral membrane protein
754 distributed in the inner leaflet cannot enter the void zone by lateral diffusion; (b) a GPI-AP,
755 Gas1, localized in the outer layer of the plasma membrane is not influenced by the void zone;
756 and (c) vacuoles move to form a stable contact with the void zone, and a vacuolar membrane
757 domain also appears to be formed at this contact site. (B) The putative structure of the void
758 zone. Our results suggest that the void zone is a Lo-like domain (see discussion).

759

760 ## Materials and Methods

761 ### Chemicals, Media, and Genetic Manipulation

Chemicals were purchased from Wako Pure Chemicals Industries (Osaka, Japan) unless indicated otherwise. Standard genetic manipulations and plasmid transformation of yeast were performed as described previously (Elble, 1992; Guthrie and Fink, 2002). Yeast strains were cultured in rich YPDA medium containing 1% yeast extract (Difco Laboratories, MI, USA), 2% Bacto peptone (Difco), 2% glucose, and 0.01% adenine, or synthetic dextrose (SD) medium containing 0.17% yeast nitrogen base w/o amino acids and ammonium sulfate (Difco), 0.5% ammonium sulfate, 2% glucose, and the required amino acids or nucleic acid bases. To induce the *GAL1* promoter, 3% galactose and 0.2% sucrose were used as carbon sources instead of glucose (YPGA medium). To deplete PS in the P_{GAL1}-*3HA-CHO1* background cells, the cells were grown on YPDA plates for more than 1 day before inoculation into YPDA medium. Strains carrying *URA3*-harbouring plasmids were cultured in SD medium containing 0.5% casamino acids (Difco), 0.03% tryptophan, and 0.01% adenine (SDA-U). When *cho1*Δ or Cho1-depleted strains were cultured in SD or SDA-U medium, ethanolamine was added to the final concentration of 1 mM. For serial dilution spot assays, cells were grown to early log phase in an appropriate medium and adjusted to a concentration of 1.0×10^7 cells/ml. After serial tenfold dilution, 4-μl drops were spotted onto appropriate plates.

Strains and Plasmids

Yeast strains and plasmids used in this study are listed in Tables 1 and 2 (Supplemental Files), respectively. Standard molecular biological techniques were used for the construction of the plasmids, PCR amplification, and DNA sequencing (Sambrook and Russell, 2001). PCR-based procedures were used to construct the gene deletions and gene fusions with GFP, mRFP, 3HA, and the *GAL1* promoter (Longtine *et al*., 1998). All constructs produced by the PCR-based procedure were verified by colony PCR to confirm that the replacement occurred

787 at the expected locus. Sequences of the PCR primers are available upon request.

788 To construct the *LEU2::mRFP-GAS1* strain, pMF608 was linearized and integrated into the
789 *LEU2* locus. To construct the pRS316-mRFP-GAS1 (pKT2191), the SacII-XmaI fragment
790 from pMF608 was inserted into the SacII-SmaI gap of pRS316. To construct pRS416-GFP-
791 GAP1C (pKT2205), the C-terminal cytoplasmic region of Gap1 corresponding to 552-602
792 amino acids (Popov-Čeleketić *et al.,* 2016) and 257 bp downstream of the *GAP1* coding
793 region were amplified by PCR, and *PEP12* region of pRS416-GFP-PEP12 (pKT1487) (Furuta
794 *et al.,* 2007) was replaced with the PCR product. To construct pRS316-mCherry-
795 SPO20PABD (pKT2206), the DNA fragments of mCherry and the PA-binding region of
796 Spo20 corresponding to 51-91 amino acids (Nakanishi *et al*., 2004) were inserted into
797 pRS316 along with P_{TPI1} and T_{ADH1}.

798

799 **Microscopic Observations**

800 Cells were observed using a Nikon ECLIPSE E800 microscope (Nikon Instec, Tokyo, Japan)
801 equipped with an HB-10103AF super-high-pressure mercury lamp and a 1.4 numerical
802 aperture 100× Plan Apo oil immersion objective lens (Nikon Instec) with appropriate
803 fluorescence filter sets (Nikon Instec) or differential interference contrast optics. Images were
804 acquired using a cooled digital charge-coupled device (CCD) camera (C4742-95-12NR;
805 Hamamatsu Photonics, Hamamatsu, Japan) and the AQUACOSMOS software (Hamamatsu
806 Photonics).

807 GFP-, mRFP-, or mCherry-tagged proteins were observed in the living cells grown in early
808 to mid-logarithmic phase, harvested, and resuspended in SD medium. Cells were immediately
809 observed using a GFP bandpass (for GFP) or a G2-A (for mRFP and mCherry) filter set.
810 Observations were compiled based on the examination of at least 100 cells. For
811 supplementation of 18:1 lyso-PS (Sigma-Aldrich, St. Louis, MO, USA), a stock solution (10

mg/mL in 0.1% Nonidet P-40) was added to the culture media to the final concentration of 20 μM. For sterol staining, cells were fixed with 5% formaldehyde, washed with PBS, and labelled for 10 min in 0.5 mg/ml filipin (Sigma-Aldrich) in PBS. For staining of the plasma membrane by FM4-64 (Thermo Fisher Scientific, MA, USA), cell suspensions were mixed with an equal volume of 100 μM FM4-64 on a glass slide and observed immediately. For staining of the vacuolar membranes, cells were labelled for 15 min in 5μM FM4-64, washed with SD medium, and immediately observed. Fluorescence of filipin and FM4-64 was observed using a UV and a G2-A filter set, respectively. For the time-lapse imaging, cell suspension was spotted onto a thin layer of SD medium containing 1 mM ethanolamine and 2% agarose on a glass slide, which was quickly covered with a coverslip. During the time-lapse imaging, the sample was maintained at 37°C by a Thermo Plate (Tokai Hit, Fujinomiya, Japan). The incidence of the void zone was assessed based on three or more images of different focal planes, and based on single focal plane in the time-lapse imaging.

Freeze-fracture replica labelling

Yeast cells sandwiched between a 20-μm–thick copper foil and a flat aluminium disc (Engineering Office M. Wohlwend, Sennwald, Switzerland) were quick-frozen by high-pressure freezing using an HPM 010 high-pressure freezing machine according to the manufacture's instruction (Leica Microsystems, Wetzlar, Germany). The frozen specimens were transferred to the cold stage of a Balzers BAF 400 apparatus and fractured at −115° to −105°C under vacuum at ~ 1×10^{-6} mbar.

For genuine morphological observation, samples were exposed to electron-beam evaporation of platinum-carbon (Pt/C) (1–2 nm thickness) at an angle of 45° to the specimen surface followed by carbon (C) (10–20 nm) at an angle of 90º. After thawing, the replicas were treated with household bleach to digest biological materials before mounting on the EM grids for

observation.

For labelling, freeze-fractured samples were subjected to a three-step electron-beam evaporation: C (2–5 nm), Pt/C (1–2 nm), and C (10–20 nm) as described previously (Fujita *et al.,* 2010). Thawed replicas were treated with 2.5% SDS in 0.1 M Tris-HCl (pH 8.0) at 60°C overnight; with 0.1% Westase (Takara Bio) in McIlvain buffer (37 mM citrate and 126 mM disodium hydrogen phosphate, pH 6.0) containing 10 mM EDTA, 30% fetal calf serum, and a protease inhibitor cocktail for 30 min at 30°C; and with 2.5% SDS in 0.1 M Tris-HCl (pH 8.0) at 60°C overnight. For labelling of GFP-Pma1, replicas were incubated at 4°C overnight with a rabbit anti-GFP antibody in PBS containing 1% BSA followed by colloidal gold (10 nm)-conjugated protein A (University of Utrecht, Utrecht, The Netherlands) for 60 min at 37°C in 1% BSA in PBS. Replicas were observed and imaged with a JEOL JEM-1011 EM (Tokyo, Japan) using a CCD camera (Gatan, Pleasanton, CA, USA).

Lipid analysis

Total lipids were extracted basically by the Bligh and Dyer method (Bligh and Dyer, 1959). Cells were grown in 100-200 ml of YPDA medium to 0.8-1.0 OD_{600}/ml at 30°C or 37°C. The cells were collected and resuspended in 3.8 ml of chloroform-methanol-0.1 M HCl/0.1 M KCl (1:2:0.8) and lysed by vortexing with glass beads for 1 min. Then, 1.0 ml each of chloroform and 0.1 M HCl/0.1 M KCl were added followed by centrifugation, isolation of the lipid-containing phase, and evaporation of the solvent. The extracted lipids were dissolved in an appropriate volume of chloroform. Total phospholipids were determined by the phosphorus assay (Rouser *et al*., 1970).

For ergosterol analysis, the samples containing 20 nmol phosphate were subjected to TLC on an HPTLC plate (Silica gel 60; Merck Millipore, MA, USA) in the solvent system hexane/diethyl ether/acetic acid (80:20:1) (Dodge and Phillips, 1967). After migration, the

plates were dried and sprayed with a 10% (w/v) cupric sulfate solution in 8% (w/v) orthophosphoric acid. Plates were heated in an oven at 180°C for 20 min. Plates were scanned with a CanoScan 8800F image scanner (Canon, Tokyo, Japan) and the acquired images were quantified using the ImageJ software.

Statistical Analysis

Significant differences in Figures 5C and 7C were determined using a two-sided Student's *t* test. Significant differences for all other figures were determined by the Tukey–Kramer test.

Acknowledgements

We thank Masahiko Watanabe (Hokkaido University, Sapporo, Japan) for providing the rabbit anti-GFP antibody for freeze-fracture replica labelling. We thank Takehiko Yoko-o (AIST, Tokyo, Japan) for providing the pMF608 plasmid. We thank our colleagues in the Tanaka laboratory for valuable discussions and Eriko Itoh for technical assistance. This work was supported by Japan Society for the Promotion of Science (JSPS) KAKENHI grants 18K14645 (T.M.), 18K06104 (T.K.), and 19K06536 (K.T.).

Competing interests

The authors have no conflict of interests to declare.

Reference

Arikketh, D., Nelson, R., & Vance, J. E. (2008). Defining the importance of phosphatidylserine synthase-1 (PSS1): unexpected viability of PSS1-deficient mice. *J Biol Chem, 283*(19), 12888-12897. doi:10.1074/jbc.M800714200

Arthington, B. A., Bennett, L. G., Skatrud, P. L., Guynn, C. J., Barbuch, R. J., Ulbright, C. E.,

& Bard, M. (1991). Cloning, disruption and sequence of the gene encoding yeast C-5 sterol desaturase. *Gene, 102*(1), 39-44. doi:10.1016/0378-1119(91)90535-j

Atkinson, K. D., Jensen, B., Kolat, A. I., Storm, E. M., Henry, S. A., & Fogel, S. (1980). Yeast mutants auxotrophic for choline or ethanolamine. *J Bacteriol, 141*(2), 558-564.

Audhya, A., & Emr, S. D. (2002). Stt4 PI 4-kinase localizes to the plasma membrane and functions in the Pkc1-mediated MAP kinase cascade. *Dev Cell, 2*(5), 593-605. doi:10.1016/s1534-5807(02)00168-5

Balderhaar, H. J., & Ungermann, C. (2013). CORVET and HOPS tethering complexes - coordinators of endosome and lysosome fusion. *J Cell Sci, 126*(Pt 6), 1307-1316. doi:10.1242/jcs.107805

Balla, T. (2013). Phosphoinositides: tiny lipids with giant impact on cell regulation. *Physiol Rev, 93*(3), 1019-1137. doi:10.1152/physrev.00028.2012

Bauer, B. E., Wolfger, H., & Kuchler, K. (1999). Inventory and function of yeast ABC proteins: about sex, stress, pleiotropic drug and heavy metal resistance. *Biochim Biophys Acta, 1461*(2), 217-236. doi:10.1016/s0005-2736(99)00160-1

Baumgart, T., Hammond, A. T., Sengupta, P., Hess, S. T., Holowka, D. A., Baird, B. A., & Webb, W. W. (2007). Large-scale fluid/fluid phase separation of proteins and lipids in giant plasma membrane vesicles. *Proc Natl Acad Sci U S A, 104*(9), 3165-3170. doi:10.1073/pnas.0611357104

Baumgart, T., Hess, S. T., & Webb, W. W. (2003). Imaging coexisting fluid domains in biomembrane models coupling curvature and line tension. *Nature, 425*(6960), 821-824. doi:10.1038/nature02013

Beh, C. T., & Rine, J. (2004). A role for yeast oxysterol-binding protein homologs in endocytosis and in the maintenance of intracellular sterol-lipid distribution. *J Cell Sci, 117*(Pt 14), 2983-2996. doi:10.1242/jcs.01157

912 Bhattacharya, S., Chen, L., Broach, J. R., & Powers, S. (1995). Ras membrane targeting is
913 essential for glucose signaling but not for viability in yeast. *Proc Natl Acad Sci U S A, 92*(7), 2984-2988. doi:10.1073/pnas.92.7.2984
914
915 Bligh, E. G., & Dyer, W. J. (1959). A rapid method of total lipid extraction and purification.
916 *Can J Biochem Physiol, 37*(8), 911-917. doi:10.1139/o59-099
917 Brett, C. L., Tukaye, D. N., Mukherjee, S., & Rao, R. (2005). The yeast endosomal
918 Na+K+/H+ exchanger Nhx1 regulates cellular pH to control vesicle trafficking. *Mol*
919 *Biol Cell, 16*(3), 1396-1405. doi:10.1091/mbc.e04-11-0999
920 Burd, C., & Cullen, P. J. (2014). Retromer: a master conductor of endosome sorting. *Cold*
921 *Spring Harb Perspect Biol, 6*(2). doi:10.1101/cshperspect.a016774
922 Carquin, M., D'Auria, L., Pollet, H., Bongarzone, E. R., & Tyteca, D. (2016). Recent progress
923 on lipid lateral heterogeneity in plasma membranes: From rafts to submicrometric
924 domains. *Prog Lipid Res, 62*, 1-24. doi:10.1016/j.plipres.2015.12.004
925 Cho, K. J., van der Hoeven, D., Zhou, Y., Maekawa, M., Ma, X., Chen, W., . . . Hancock, J.
926 F. (2015). Inhibition of Acid Sphingomyelinase Depletes Cellular Phosphatidylserine
927 and Mislocalizes K-Ras from the Plasma Membrane. *Mol Cell Biol, 36*(2), 363-374.
928 doi:10.1128/mcb.00719-15
929 Collado, J., Kalemanov, M., Campelo, F., Bourgoint, C., Thomas, F., Loewith, R., . . .
930 Fernández-Busnadiego, R. (2019). Tricalbin-Mediated Contact Sites Control ER
931 Curvature to Maintain Plasma Membrane Integrity. *Dev Cell, 51*(4), 476-487.e477.
932 doi:10.1016/j.devcel.2019.10.018
933 Cooke, F. T., Dove, S. K., McEwen, R. K., Painter, G., Holmes, A. B., Hall, M. N., . . .
934 Parker, P. J. (1998). The stress-activated phosphatidylinositol 3-phosphate 5-kinase
935 Fab1p is essential for vacuole function in S. cerevisiae. *Curr Biol, 8*(22), 1219-1222.
936 doi:10.1016/s0960-9822(07)00513-1

Cordeiro, R. M. (2018). Molecular Structure and Permeability at the Interface between Phase-Separated Membrane Domains. *J Phys Chem B, 122*(27), 6954-6965. doi:10.1021/acs.jpcb.8b03406

Courtney, K. C., Pezeshkian, W., Raghupathy, R., Zhang, C., Darbyson, A., Ipsen, J. H., . . . Zha, X. (2018). C24 Sphingolipids Govern the Transbilayer Asymmetry of Cholesterol and Lateral Organization of Model and Live-Cell Plasma Membranes. *Cell Rep, 24*(4), 1037-1049. doi:10.1016/j.celrep.2018.06.104

Dawaliby, R., & Mayer, A. (2010). Microautophagy of the nucleus coincides with a vacuolar diffusion barrier at nuclear-vacuolar junctions. *Mol Biol Cell, 21*(23), 4173-4183. doi:10.1091/mbc.E09-09-0782

de Almeida, R. F., Fedorov, A., & Prieto, M. (2003). Sphingomyelin/phosphatidylcholine/cholesterol phase diagram: boundaries and composition of lipid rafts. *Biophys J, 85*(4), 2406-2416. doi:10.1016/s0006-3495(03)74664-5

De Craene, J. O., Coleman, J., Estrada de Martin, P., Pypaert, M., Anderson, S., Yates, J. R., 3rd, . . . Novick, P. (2006). Rtn1p is involved in structuring the cortical endoplasmic reticulum. *Mol Biol Cell, 17*(7), 3009-3020. doi:10.1091/mbc.e06-01-0080

de Saint-Jean, M., Delfosse, V., Douguet, D., Chicanne, G., Payrastre, B., Bourguet, W., . . . Drin, G. (2011). Osh4p exchanges sterols for phosphatidylinositol 4-phosphate between lipid bilayers. *J Cell Biol, 195*(6), 965-978. doi:10.1083/jcb.201104062

Dechant, R., Binda, M., Lee, S. S., Pelet, S., Winderickx, J., & Peter, M. (2010). Cytosolic pH is a second messenger for glucose and regulates the PKA pathway through V-ATPase. *Embo j, 29*(15), 2515-2526. doi:10.1038/emboj.2010.138

Dell'Angelica, E. C. (2009). AP-3-dependent trafficking and disease: the first decade. *Curr Opin Cell Biol, 21*(4), 552-559. doi:10.1016/j.ceb.2009.04.014

962 Dickson, R. C., Nagiec, E. E., Wells, G. B., Nagiec, M. M., & Lester, R. L. (1997). Synthesis
963 of mannose-(inositol-P)2-ceramide, the major sphingolipid in Saccharomyces
964 cerevisiae, requires the IPT1 (YDR072c) gene. *J Biol Chem, 272*(47), 29620-29625.
965 doi:10.1074/jbc.272.47.29620
966 Dietrich, C., Bagatolli, L. A., Volovyk, Z. N., Thompson, N. L., Levi, M., Jacobson, K., &
967 Gratton, E. (2001). Lipid rafts reconstituted in model membranes. *Biophys J, 80*(3),
968 1417-1428. doi:10.1016/s0006-3495(01)76114-0
969 Dodge, J. T., & Phillips, G. B. (1967). Composition of phospholipids and of phospholipid
970 fatty acids and aldehydes in human red cells. *J Lipid Res, 8*(6), 667-675.
971 Douglas, L. M., & Konopka, J. B. (2014). Fungal membrane organization: the eisosome
972 concept. *Annu Rev Microbiol, 68*, 377-393. doi:10.1146/annurev-micro-091313-
973 103507
974 Ejsing, C. S., Sampaio, J. L., Surendranath, V., Duchoslav, E., Ekroos, K., Klemm, R. W., . . .
975 Shevchenko, A. (2009). Global analysis of the yeast lipidome by quantitative shotgun
976 mass spectrometry. *Proc Natl Acad Sci U S A, 106*(7), 2136-2141.
977 doi:10.1073/pnas.0811700106
978 Elble, R. (1992). A simple and efficient procedure for transformation of yeasts.
979 *Biotechniques, 13*(1), 18-20.
980 Elson, E. L., Fried, E., Dolbow, J. E., & Genin, G. M. (2010). Phase separation in biological
981 membranes: integration of theory and experiment. *Annu Rev Biophys, 39*, 207-226.
982 doi:10.1146/annurev.biophys.093008.131238
983 Engberg, O., Hautala, V., Yasuda, T., Dehio, H., Murata, M., Slotte, J. P., & Nyholm, T. K.
984 M. (2016). The Affinity of Cholesterol for Different Phospholipids Affects Lateral
985 Segregation in Bilayers. *Biophys J, 111*(3), 546-556. doi:10.1016/j.bpj.2016.06.036
986 Fairn, G. D., Hermansson, M., Somerharju, P., & Grinstein, S. (2011). Phosphatidylserine is

polarized and required for proper Cdc42 localization and for development of cell polarity. *Nat Cell Biol, 13*(12), 1424-1430. doi:10.1038/ncb2351

Fischer, M. A., Temmerman, K., Ercan, E., Nickel, W., & Seedorf, M. (2009). Binding of plasma membrane lipids recruits the yeast integral membrane protein Ist2 to the cortical ER. *Traffic, 10*(8), 1084-1097. doi:10.1111/j.1600-0854.2009.00926.x

Fujita, A., Cheng, J., & Fujimoto, T. (2010). Quantitative electron microscopy for the nanoscale analysis of membrane lipid distribution. *Nat Protoc, 5*(4), 661-669. doi:10.1038/nprot.2010.20

Fujita, M., & Kinoshita, T. (2012). GPI-anchor remodeling: potential functions of GPI-anchors in intracellular trafficking and membrane dynamics. *Biochim Biophys Acta, 1821*(8), 1050-1058. doi:10.1016/j.bbalip.2012.01.004

Furuta, N., Fujimura-Kamada, K., Saito, K., Yamamoto, T., & Tanaka, K. (2007). Endocytic recycling in yeast is regulated by putative phospholipid translocases and the Ypt31p/32p-Rcy1p pathway. *Mol Biol Cell, 18*(1), 295-312. doi:10.1091/mbc.e06-05-0461

García-Arribas, A. B., Alonso, A., & Goñi, F. M. (2016). Cholesterol interactions with ceramide and sphingomyelin. *Chem Phys Lipids, 199*, 26-34. doi:10.1016/j.chemphyslip.2016.04.002

Georgiev, A. G., Johansen, J., Ramanathan, V. D., Sere, Y. Y., Beh, C. T., & Menon, A. K. (2013). Arv1 regulates PM and ER membrane structure and homeostasis but is dispensable for intracellular sterol transport. *Traffic, 14*(8), 912-921. doi:10.1111/tra.12082

Georgiev, A. G., Sullivan, D. P., Kersting, M. C., Dittman, J. S., Beh, C. T., & Menon, A. K. (2011). Osh proteins regulate membrane sterol organization but are not required for sterol movement between the ER and PM. *Traffic, 12*(10), 1341-1355.

doi:10.1111/j.1600-0854.2011.01234.x

Giménez-Andrés, M., Čopič, A., & Antonny, B. (2018). The Many Faces of Amphipathic Helices. *Biomolecules, 8*(3). doi:10.3390/biom8030045

Goñi, F. M., & Alonso, A. (2009). Effects of ceramide and other simple sphingolipids on membrane lateral structure. *Biochim Biophys Acta, 1788*(1), 169-177. doi:10.1016/j.bbamem.2008.09.002

Gray, J. V., Petsko, G. A., Johnston, G. C., Ringe, D., Singer, R. A., & Werner-Washburne, M. (2004). "Sleeping beauty": quiescence in Saccharomyces cerevisiae. *Microbiol Mol Biol Rev, 68*(2), 187-206. doi:10.1128/mmbr.68.2.187-206.2004

Grossmann, G., Opekarová, M., Malinsky, J., Weig-Meckl, I., & Tanner, W. (2007). Membrane potential governs lateral segregation of plasma membrane proteins and lipids in yeast. *Embo j, 26*(1), 1-8. doi:10.1038/sj.emboj.7601466

Guthrie, C., Fink, GR. (2002). Guide to Yeast Genetics and Molecular Biology, San Diego: Academic Press.

Haak, D., Gable, K., Beeler, T., & Dunn, T. (1997). Hydroxylation of Saccharomyces cerevisiae ceramides requires Sur2p and Scs7p. *J Biol Chem, 272*(47), 29704-29710. doi:10.1074/jbc.272.47.29704

Jiang, B., Brown, J. L., Sheraton, J., Fortin, N., & Bussey, H. (1994). A new family of yeast genes implicated in ergosterol synthesis is related to the human oxysterol binding protein. *Yeast, 10*(3), 341-353. doi:10.1002/yea.320100307

Jin, N., Lang, M. J., & Weisman, L. S. (2016). Phosphatidylinositol 3,5-bisphosphate: regulation of cellular events in space and time. *Biochem Soc Trans, 44*(1), 177-184. doi:10.1042/bst20150174

Kaiser, H. J., Lingwood, D., Levental, I., Sampaio, J. L., Kalvodova, L., Rajendran, L., & Simons, K. (2009). Order of lipid phases in model and plasma membranes. *Proc Natl*

Acad Sci U S A, 106(39), 16645-16650. doi:10.1073/pnas.0908987106

Kajiwara, K., Watanabe, R., Pichler, H., Ihara, K., Murakami, S., Riezman, H., & Funato, K. (2008). Yeast ARV1 is required for efficient delivery of an early GPI intermediate to the first mannosyltransferase during GPI assembly and controls lipid flow from the endoplasmic reticulum. *Mol Biol Cell, 19*(5), 2069-2082. doi:10.1091/mbc.e07-08-0740

Kamiński, D. M. (2014). Recent progress in the study of the interactions of amphotericin B with cholesterol and ergosterol in lipid environments. *Eur Biophys J, 43*(10-11), 453-467. doi:10.1007/s00249-014-0983-8

Kato, U., Emoto, K., Fredriksson, C., Nakamura, H., Ohta, A., Kobayashi, T., . . . Umeda, M. (2002). A novel membrane protein, Ros3p, is required for phospholipid translocation across the plasma membrane in Saccharomyces cerevisiae. *J Biol Chem, 277*(40), 37855-37862. doi:10.1074/jbc.M205564200

Klose, C., Ejsing, C. S., García-Sáez, A. J., Kaiser, H. J., Sampaio, J. L., Surma, M. A., . . . Simons, K. (2010). Yeast lipids can phase-separate into micrometer-scale membrane domains. *J Biol Chem, 285*(39), 30224-30232. doi:10.1074/jbc.M110.123554

Klose, C., Surma, M. A., Gerl, M. J., Meyenhofer, F., Shevchenko, A., & Simons, K. (2012). Flexibility of a eukaryotic lipidome--insights from yeast lipidomics. *PLoS One, 7*(4), e35063. doi:10.1371/journal.pone.0035063

Koning, A. J., Roberts, C. J., & Wright, R. L. (1996). Different subcellular localization of Saccharomyces cerevisiae HMG-CoA reductase isozymes at elevated levels corresponds to distinct endoplasmic reticulum membrane proliferations. *Mol Biol Cell, 7*(5), 769-789. doi:10.1091/mbc.7.5.769

Krauss, M., Jia, J. Y., Roux, A., Beck, R., Wieland, F. T., De Camilli, P., & Haucke, V. (2008). Arf1-GTP-induced tubule formation suggests a function of Arf family proteins

in curvature acquisition at sites of vesicle budding. *J Biol Chem, 283*(41), 27717-27723. doi:10.1074/jbc.M804528200

Kusumi, A., Fujiwara, T. K., Chadda, R., Xie, M., Tsunoyama, T. A., Kalay, Z., . . . Suzuki, K. G. (2012). Dynamic organizing principles of the plasma membrane that regulate signal transduction: commemorating the fortieth anniversary of Singer and Nicolson's fluid-mosaic model. *Annu Rev Cell Dev Biol, 28*, 215-250. doi:10.1146/annurev-cellbio-100809-151736

Lai, M. H., Bard, M., Pierson, C. A., Alexander, J. F., Goebl, M., Carter, G. T., & Kirsch, D. R. (1994). The identification of a gene family in the Saccharomyces cerevisiae ergosterol biosynthesis pathway. *Gene, 140*(1), 41-49. doi:10.1016/0378-1119(94)90728-5

Lemmon, M. A., Ferguson, K. M., O'Brien, R., Sigler, P. B., & Schlessinger, J. (1995). Specific and high-affinity binding of inositol phosphates to an isolated pleckstrin homology domain. *Proc Natl Acad Sci U S A, 92*(23), 10472-10476. doi:10.1073/pnas.92.23.10472

Levental, I., Byfield, F. J., Chowdhury, P., Gai, F., Baumgart, T., & Janmey, P. A. (2009). Cholesterol-dependent phase separation in cell-derived giant plasma-membrane vesicles. *Biochem J, 424*(2), 163-167. doi:10.1042/bj20091283

Lewis, M. J., Nichols, B. J., Prescianotto-Baschong, C., Riezman, H., & Pelham, H. R. (2000). Specific retrieval of the exocytic SNARE Snc1p from early yeast endosomes. *Mol Biol Cell, 11*(1), 23-38. doi:10.1091/mbc.11.1.23

Li, B., & Warner, J. R. (1996). Mutation of the Rab6 homologue of Saccharomyces cerevisiae, YPT6, inhibits both early Golgi function and ribosome biosynthesis. *J Biol Chem, 271*(28), 16813-16819. doi:10.1074/jbc.271.28.16813

Li, L., & Kaplan, J. (1998). Defects in the yeast high affinity iron transport system result in

increased metal sensitivity because of the increased expression of transporters with a broad transition metal specificity. *J Biol Chem, 273*(35), 22181-22187. doi:10.1074/jbc.273.35.22181

Lingwood, D., & Simons, K. (2010). Lipid rafts as a membrane-organizing principle. *Science, 327*(5961), 46-50. doi:10.1126/science.1174621

Longtine, M. S., McKenzie, A., 3rd, Demarini, D. J., Shah, N. G., Wach, A., Brachat, A., . . . Pringle, J. R. (1998). Additional modules for versatile and economical PCR-based gene deletion and modification in Saccharomyces cerevisiae. *Yeast, 14*(10), 953-961. doi:10.1002/(sici)1097-0061(199807)14:10<953::aid-yea293>3.0.co;2-u

López-Montero, I., Monroy, F., Vélez, M., & Devaux, P. F. (2010). Ceramide: from lateral segregation to mechanical stress. *Biochim Biophys Acta, 1798*(7), 1348-1356. doi:10.1016/j.bbamem.2009.12.007

Maeda, K., Anand, K., Chiapparino, A., Kumar, A., Poletto, M., Kaksonen, M., & Gavin, A. C. (2013). Interactome map uncovers phosphatidylserine transport by oxysterol-binding proteins. *Nature, 501*(7466), 257-261. doi:10.1038/nature12430

Maekawa, M., & Fairn, G. D. (2015). Complementary probes reveal that phosphatidylserine is required for the proper transbilayer distribution of cholesterol. *J Cell Sci, 128*(7), 1422-1433. doi:10.1242/jcs.164715

Manneville, J. B., Casella, J. F., Ambroggio, E., Gounon, P., Bertherat, J., Bassereau, P., . . . Goud, B. (2008). COPI coat assembly occurs on liquid-disordered domains and the associated membrane deformations are limited by membrane tension. *Proc Natl Acad Sci U S A, 105*(44), 16946-16951. doi:10.1073/pnas.0807102105

Manolson, M. F., Proteau, D., Preston, R. A., Stenbit, A., Roberts, B. T., Hoyt, M. A., . . . Jones, E. W. (1992). The VPH1 gene encodes a 95-kDa integral membrane polypeptide required for in vivo assembly and activity of the yeast vacuolar H(+)-

ATPase. *J Biol Chem, 267*(20), 14294-14303.

Marshansky, V., Rubinstein, J. L., & Grüber, G. (2014). Eukaryotic V-ATPase: novel structural findings and functional insights. *Biochim Biophys Acta, 1837*(6), 857-879. doi:10.1016/j.bbabio.2014.01.018

Michell, R. H. (2008). Inositol derivatives: evolution and functions. *Nat Rev Mol Cell Biol, 9*(2), 151-161. doi:10.1038/nrm2334

Middel, V., Zhou, L., Takamiya, M., Beil, T., Shahid, M., Roostalu, U., . . . Strähle, U. (2016). Dysferlin-mediated phosphatidylserine sorting engages macrophages in sarcolemma repair. *Nat Commun, 7*, 12875. doi:10.1038/ncomms12875

Mioka, T., Fujimura-Kamada, K., Mizugaki, N., Kishimoto, T., Sano, T., Nunome, H., . . . Tanaka, K. (2018). Phospholipid flippases and Sfk1p, a novel regulator of phospholipid asymmetry, contribute to low permeability of the plasma membrane. *Mol Biol Cell, 29*(10), 1203-1218. doi:10.1091/mbc.E17-04-0217

Mizushima, N., Yoshimori, T., & Ohsumi, Y. (2011). The role of Atg proteins in autophagosome formation. *Annu Rev Cell Dev Biol, 27*, 107-132. doi:10.1146/annurev-cellbio-092910-154005

Morvan, J., de Craene, J. O., Rinaldi, B., Addis, V., Misslin, C., & Friant, S. (2015). Btn3 regulates the endosomal sorting function of the yeast Ent3 epsin, an adaptor for SNARE proteins. *J Cell Sci, 128*(4), 706-716. doi:10.1242/jcs.159699

Muñiz, M., & Zurzolo, C. (2014). Sorting of GPI-anchored proteins from yeast to mammals--common pathways at different sites? *J Cell Sci, 127*(Pt 13), 2793-2801. doi:10.1242/jcs.148056

Nakanishi, H., de los Santos, P., & Neiman, A. M. (2004). Positive and negative regulation of a SNARE protein by control of intracellular localization. *Mol Biol Cell, 15*(4), 1802-1815. doi:10.1091/mbc.e03-11-0798

1137 Nicolson, G. L. (2014). The Fluid-Mosaic Model of Membrane Structure: still relevant to
1138 understanding the structure, function and dynamics of biological membranes after
1139 more than 40 years. *Biochim Biophys Acta, 1838*(6), 1451-1466.
1140 doi:10.1016/j.bbamem.2013.10.019
1141 Nuoffer, C., Jenö, P., Conzelmann, A., & Riezman, H. (1991). Determinants for
1142 glycophospholipid anchoring of the Saccharomyces cerevisiae GAS1 protein to the
1143 plasma membrane. *Mol Cell Biol, 11*(1), 27-37. doi:10.1128/mcb.11.1.27
1144 Nyholm, T. K. M., Jaikishan, S., Engberg, O., Hautala, V., & Slotte, J. P. (2019). The Affinity
1145 of Sterols for Different Phospholipid Classes and Its Impact on Lateral Segregation.
1146 *Biophys J, 116*(2), 296-307. doi:10.1016/j.bpj.2018.11.3135
1147 Obara, K., Yamamoto, H., & Kihara, A. (2012). Membrane protein Rim21 plays a central role
1148 in sensing ambient pH in Saccharomyces cerevisiae. *J Biol Chem, 287*(46), 38473-
1149 38481. doi:10.1074/jbc.M112.394205
1150 Oh, C. S., Toke, D. A., Mandala, S., & Martin, C. E. (1997). ELO2 and ELO3, homologues of
1151 the Saccharomyces cerevisiae ELO1 gene, function in fatty acid elongation and are
1152 required for sphingolipid formation. *J Biol Chem, 272*(28), 17376-17384.
1153 doi:10.1074/jbc.272.28.17376
1154 Omnus, D. J., Manford, A. G., Bader, J. M., Emr, S. D., & Stefan, C. J. (2016).
1155 Phosphoinositide kinase signaling controls ER-PM cross-talk. *Mol Biol Cell, 27*(7),
1156 1170-1180. doi:10.1091/mbc.E16-01-0002
1157 Pan, X., Roberts, P., Chen, Y., Kvam, E., Shulga, N., Huang, K., . . . Goldfarb, D. S. (2000).
1158 Nucleus-vacuole junctions in Saccharomyces cerevisiae are formed through the direct
1159 interaction of Vac8p with Nvj1p. *Mol Biol Cell, 11*(7), 2445-2457.
1160 doi:10.1091/mbc.11.7.2445
1161 Pittet, M., & Conzelmann, A. (2007). Biosynthesis and function of GPI proteins in the yeast

1162 Saccharomyces cerevisiae. *Biochim Biophys Acta, 1771*(3), 405-420.
1163 doi:10.1016/j.bbalip.2006.05.015
1164 Plasencia, I., Norlén, L., & Bagatolli, L. A. (2007). Direct visualization of lipid domains in
1165 human skin stratum corneum's lipid membranes: effect of pH and temperature.
1166 *Biophys J, 93*(9), 3142-3155. doi:10.1529/biophysj.106.096164
1167 Pomorski, T., Lombardi, R., Riezman, H., Devaux, P. F., van Meer, G., & Holthuis, J. C.
1168 (2003). Drs2p-related P-type ATPases Dnf1p and Dnf2p are required for phospholipid
1169 translocation across the yeast plasma membrane and serve a role in endocytosis. *Mol*
1170 *Biol Cell, 14*(3), 1240-1254. doi:10.1091/mbc.e02-08-0501
1171 Popov-Čeleketić, D., Bianchi, F., Ruiz, S. J., Meutiawati, F., & Poolman, B. (2016). A Plasma
1172 Membrane Association Module in Yeast Amino Acid Transporters. *J Biol Chem,*
1173 *291*(31), 16024-16037. doi:10.1074/jbc.M115.706770
1174 Quon, E., Sere, Y. Y., Chauhan, N., Johansen, J., Sullivan, D. P., Dittman, J. S., . . . Menon,
1175 A. K. (2018). Endoplasmic reticulum-plasma membrane contact sites integrate sterol
1176 and phospholipid regulation. *PLoS Biol, 16*(5), e2003864.
1177 doi:10.1371/journal.pbio.2003864
1178 Risselada, H. J., & Marrink, S. J. (2008). The molecular face of lipid rafts in model
1179 membranes. *Proc Natl Acad Sci U S A, 105*(45), 17367-17372.
1180 doi:10.1073/pnas.0807527105
1181 Robinson, J. S., Klionsky, D. J., Banta, L. M., & Emr, S. D. (1988). Protein sorting in
1182 Saccharomyces cerevisiae: isolation of mutants defective in the delivery and
1183 processing of multiple vacuolar hydrolases. *Mol Cell Biol, 8*(11), 4936-4948.
1184 doi:10.1128/mcb.8.11.4936
1185 Rosenwald, A. G., Rhodes, M. A., Van Valkenburgh, H., Palanivel, V., Chapman, G., Boman,
1186 A., . . . Kahn, R. A. (2002). ARL1 and membrane traffic in Saccharomyces cerevisiae.

Yeast, 19(12), 1039-1056. doi:10.1002/yea.897

Rothman, J. H., Howald, I., & Stevens, T. H. (1989). Characterization of genes required for protein sorting and vacuolar function in the yeast Saccharomyces cerevisiae. *Embo j, 8*(7), 2057-2065.

Rouser, G., Fkeischer, S., & Yamamoto, A. (1970). Two dimensional then layer chromatographic separation of polar lipids and determination of phospholipids by phosphorus analysis of spots. *Lipids, 5*(5), 494-496. doi:10.1007/bf02531316

Roy, A., & Levine, T. P. (2004). Multiple pools of phosphatidylinositol 4-phosphate detected using the pleckstrin homology domain of Osh2p. *J Biol Chem, 279*(43), 44683-44689. doi:10.1074/jbc.M401583200

Saheki, Y., & De Camilli, P. (2017). Endoplasmic Reticulum-Plasma Membrane Contact Sites. *Annu Rev Biochem, 86*, 659-684. doi:10.1146/annurev-biochem-061516-044932

Saito, K., Fujimura-Kamada, K., Furuta, N., Kato, U., Umeda, M., & Tanaka, K. (2004). Cdc50p, a protein required for polarized growth, associates with the Drs2p P-type ATPase implicated in phospholipid translocation in Saccharomyces cerevisiae. *Mol Biol Cell, 15*(7), 3418-3432. doi:10.1091/mbc.e03-11-0829

Sakane, H., Yamamoto, T., & Tanaka, K. (2006). The functional relationship between the Cdc50p-Drs2p putative aminophospholipid translocase and the Arf GAP Gcs1p in vesicle formation in the retrieval pathway from yeast early endosomes to the TGN. *Cell Struct Funct, 31*(2), 87-108. doi:10.1247/csf.06021

Sambrook, J., Russell, DW. (2001). Molecular Cloning: A Laboratory Manual, Cold Spring Harbor, NY: Cold Spring Harbor Laboratory Press.

Schmidt, O., & Teis, D. (2012). The ESCRT machinery. *Curr Biol, 22*(4), R116-120. doi:10.1016/j.cub.2012.01.028

Schneiter, R., Brügger, B., Sandhoff, R., Zellnig, G., Leber, A., Lampl, M., . . . Kohlwein, S.

1212 D. (1999). Electrospray ionization tandem mass spectrometry (ESI-MS/MS) analysis
1213 of the lipid molecular species composition of yeast subcellular membranes reveals
1214 acyl chain-based sorting/remodeling of distinct molecular species en route to the
1215 plasma membrane. *J Cell Biol, 146*(4), 741-754. doi:10.1083/jcb.146.4.741
1216 Schulz, T. A., & Creutz, C. E. (2004). The tricalbin C2 domains: lipid-binding properties of a
1217 novel, synaptotagmin-like yeast protein family. *Biochemistry, 43*(13), 3987-3995.
1218 doi:10.1021/bi036082w
1219 Schäfer, L. V., de Jong, D. H., Holt, A., Rzepiela, A. J., de Vries, A. H., Poolman, B., . . .
1220 Marrink, S. J. (2011). Lipid packing drives the segregation of transmembrane helices
1221 into disordered lipid domains in model membranes. *Proc Natl Acad Sci U S A, 108*(4),
1222 1343-1348. doi:10.1073/pnas.1009362108
1223 Sengupta, P., Hammond, A., Holowka, D., & Baird, B. (2008). Structural determinants for
1224 partitioning of lipids and proteins between coexisting fluid phases in giant plasma
1225 membrane vesicles. *Biochim Biophys Acta, 1778*(1), 20-32.
1226 doi:10.1016/j.bbamem.2007.08.028
1227 Serrano, R., Kielland-Brandt, M. C., & Fink, G. R. (1986). Yeast plasma membrane ATPase
1228 is essential for growth and has homology with (Na+ + K+), K+- and Ca2+-ATPases.
1229 *Nature, 319*(6055), 689-693. doi:10.1038/319689a0
1230 Sharma, P., Varma, R., Sarasij, R. C., Ira, Gousset, K., Krishnamoorthy, G., . . . Mayor, S.
1231 (2004). Nanoscale organization of multiple GPI-anchored proteins in living cell
1232 membranes. *Cell, 116*(4), 577-589. doi:10.1016/s0092-8674(04)00167-9
1233 Silve, S., Dupuy, P. H., Labit-Lebouteiller, C., Kaghad, M., Chalon, P., Rahier, A., . . .
1234 Loison, G. (1996). Emopamil-binding protein, a mammalian protein that binds a series
1235 of structurally diverse neuroprotective agents, exhibits delta8-delta7 sterol isomerase
1236 activity in yeast. *J Biol Chem, 271*(37), 22434-22440. doi:10.1074/jbc.271.37.22434

1237 Singer, S. J., & Nicolson, G. L. (1972). The fluid mosaic model of the structure of cell
1238 membranes. *Science, 175*(4023), 720-731. doi:10.1126/science.175.4023.720
1239 Solanko, L. M., Sullivan, D. P., Sere, Y. Y., Szomek, M., Lunding, A., Solanko, K. A., . . .
1240 Wüstner, D. (2018). Ergosterol is mainly located in the cytoplasmic leaflet of the yeast
1241 plasma membrane. *Traffic, 19*(3), 198-214. doi:10.1111/tra.12545
1242 Sychrová, H., Ramírez, J., & Peña, A. (1999). Involvement of Nha1 antiporter in regulation of
1243 intracellular pH in Saccharomyces cerevisiae. *FEMS Microbiol Lett, 171*(2), 167-172.
1244 doi:10.1111/j.1574-6968.1999.tb13428.x
1245 Toulmay, A., & Prinz, W. A. (2013). Direct imaging reveals stable, micrometer-scale lipid
1246 domains that segregate proteins in live cells. *J Cell Biol, 202*(1), 35-44.
1247 doi:10.1083/jcb.201301039
1248 Trimble, W. S., & Grinstein, S. (2015). Barriers to the free diffusion of proteins and lipids in
1249 the plasma membrane. *J Cell Biol, 208*(3), 259-271. doi:10.1083/jcb.201410071
1250 Tsuchiya, M., Hara, Y., Okuda, M., Itoh, K., Nishioka, R., Shiomi, A., . . . Umeda, M. (2018).
1251 Cell surface flip-flop of phosphatidylserine is critical for PIEZO1-mediated myotube
1252 formation. *Nat Commun, 9*(1), 2049. doi:10.1038/s41467-018-04436-w
1253 Tsuji, T., Fujimoto, M., Tatematsu, T., Cheng, J., Orii, M., Takatori, S., & Fujimoto, T.
1254 (2017). Niemann-Pick type C proteins promote microautophagy by expanding raft-like
1255 membrane domains in the yeast vacuole. *Elife, 6*. doi:10.7554/eLife.25960
1256 Uchida, Y., Hasegawa, J., Chinnapen, D., Inoue, T., Okazaki, S., Kato, R., . . . Arai, H.
1257 (2011). Intracellular phosphatidylserine is essential for retrograde membrane traffic
1258 through endosomes. *Proc Natl Acad Sci U S A, 108*(38), 15846-15851.
1259 doi:10.1073/pnas.1109101108
1260 van Leeuwen, J., Pons, C., Mellor, J. C., Yamaguchi, T. N., Friesen, H., Koschwanez, J., . . .
1261 Boone, C. (2016). Exploring genetic suppression interactions on a global scale.

Science, 354(6312). doi:10.1126/science.aag0839

Vater, C. A., Raymond, C. K., Ekena, K., Howald-Stevenson, I., & Stevens, T. H. (1992). The VPS1 protein, a homolog of dynamin required for vacuolar protein sorting in Saccharomyces cerevisiae, is a GTPase with two functionally separable domains. *J Cell Biol, 119*(4), 773-786. doi:10.1083/jcb.119.4.773

Veatch, S. L., & Keller, S. L. (2003). Separation of liquid phases in giant vesicles of ternary mixtures of phospholipids and cholesterol. *Biophys J, 85*(5), 3074-3083. doi:10.1016/s0006-3495(03)74726-2

Wang, C. W., Miao, Y. H., & Chang, Y. S. (2014). A sterol-enriched vacuolar microdomain mediates stationary phase lipophagy in budding yeast. *J Cell Biol, 206*(3), 357-366. doi:10.1083/jcb.201404115

Watt, S. A., Kular, G., Fleming, I. N., Downes, C. P., & Lucocq, J. M. (2002). Subcellular localization of phosphatidylinositol 4,5-bisphosphate using the pleckstrin homology domain of phospholipase C delta1. *Biochem J, 363*(Pt 3), 657-666. doi:10.1042/0264-6021:3630657

Wells, G. B., Dickson, R. C., & Lester, R. L. (1998). Heat-induced elevation of ceramide in Saccharomyces cerevisiae via de novo synthesis. *J Biol Chem, 273*(13), 7235-7243. doi:10.1074/jbc.273.13.7235

Yamamoto, T., Fujimura-Kamada, K., Shioji, E., Suzuki, R., & Tanaka, K. (2017). Cfs1p, a Novel Membrane Protein in the PQ-Loop Family, Is Involved in Phospholipid Flippase Functions in Yeast. *G3 (Bethesda), 7*(1), 179-192. doi:10.1534/g3.116.035238

Yeung, B. G., Phan, H. L., & Payne, G. S. (1999). Adaptor complex-independent clathrin function in yeast. *Mol Biol Cell, 10*(11), 3643-3659. doi:10.1091/mbc.10.11.3643

Yeung, T., Gilbert, G. E., Shi, J., Silvius, J., Kapus, A., & Grinstein, S. (2008). Membrane

phosphatidylserine regulates surface charge and protein localization. *Science, 319*(5860), 210-213. doi:10.1126/science.1152066

Young, B. P., Shin, J. J., Orij, R., Chao, J. T., Li, S. C., Guan, X. L., . . . Loewen, C. J. (2010). Phosphatidic acid is a pH biosensor that links membrane biogenesis to metabolism. *Science, 329*(5995), 1085-1088. doi:10.1126/science.1191026